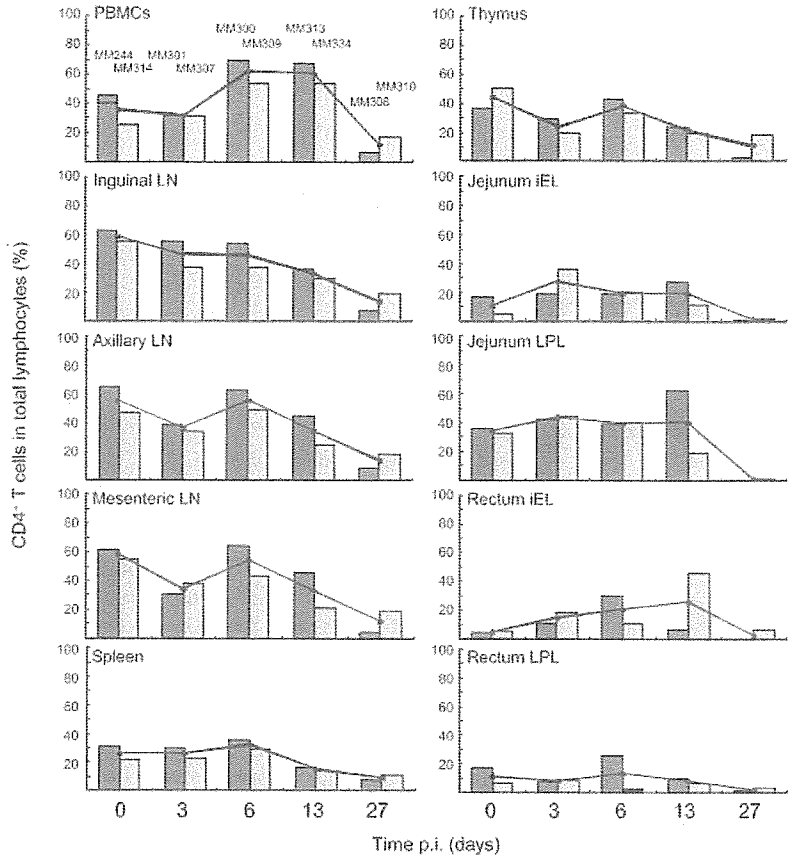

Fig. 5. Sequential changes in the proportion of $CD4^+$ T cells in the various tissues early after intrarectal infection. The percentage of $CD4^+$ T cells in total lymphocytes was determined by flow cytometry. Each bar represents one monkey. The lines indicate the mean values of two monkeys at each time point.

suggest that there is a difference in the effect of virus infection on CD4 SP T cells, CD4CD8 DP T cells and $CD3^-$CD4CD8 DP cells early after intrarectal infection.

DISCUSSION

In this study, to observe the early virological events in various tissues after mucosal infection, SHIV-C2/1-KS661c was used to inoculate rhesus monkeys intrarectally and proviral DNA and infectious viruses were quantified in various tissues by quantitative PCR and infectious plaque assay, respectively. At 3 days p.i., proviral DNA was already present in not only the rectum, but also the thymus, axillary lymph node, kidney and lung. These results suggested that the intrarectally inoculated virus spread quickly to the systemic tissues. Hu *et al.* (2000) showed that SIV penetrated the vaginal mucosa of rhesus macaques within 60 min of intravaginal inoculation, infecting primarily intraepithelial

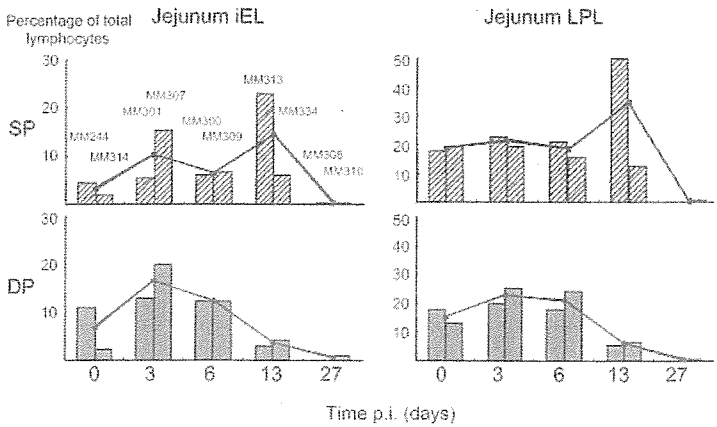

Fig. 6. Sequential changes in the proportion of CD4 single-positive (SP) and CD4CD8 double-positive (DP) T cells in the jejunum iEL and LPL. The percentage of $CD4^+$ T cells in total lymphocytes was determined by flow cytometry. Each bar represents one monkey. The lines indicate the mean values of two monkeys at each time point.

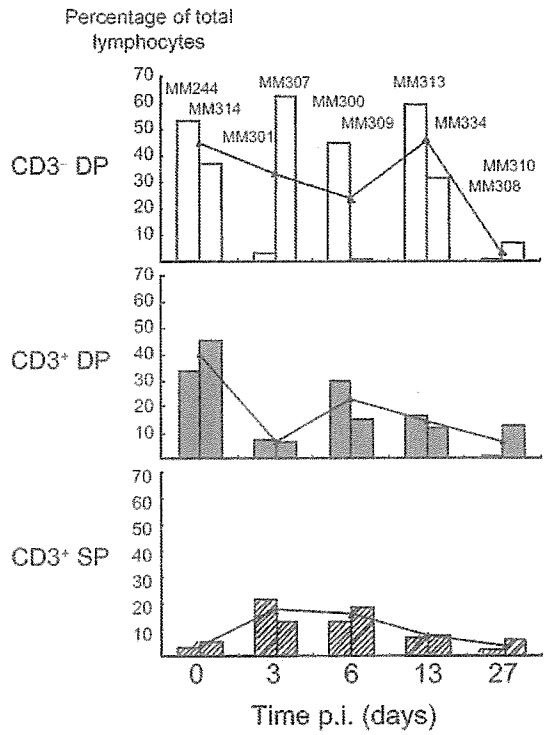

Fig. 7. Sequential changes in the proportion of CD4 single-positive (SP) and CD4CD8 double-positive (DP) T cells in the thymus. The percentage of $CD4^+$ T cells in total lymphocytes was determined by flow cytometry. Each bar represents one monkey. The lines indicate the mean values of two monkeys at each time point.

dendritic cells (DCs), and that SIV-infected cells were detected in iliac lymph nodes within 18 h of inoculation. Because the epithelium of the rectum mucosa is just as rich in DCs as the vaginal mucosa, it appears that the virus is transported to the draining lymph nodes by DCs within several hours of intrarectal exposure in this study. Once the virus reaches the local lymphoid tissues, systemic dissemination might occur shortly thereafter.

Virus levels increased remarkably between 6 and 13 days p.i. and high levels of proviral DNA and infectious virus were detected in various lymphoid tissues at 13 days p.i., which was the time of peak viraemia. Among all the tissues examined, the mesenteric lymph node had the largest level of infectious virus. This result is consistent with a previous study that showed that mesenteric lymph nodes contain numerous SIV-infected cells in the early stages of SIV infection (Cantó-Nogués *et al.*, 2001; O'Neil *et al.*, 1999). The intestinal tract is constantly exposed to antigens in foods and pathogens. Therefore, the mesenteric lymph node, which is a draining lymph node of the intestinal tract, might have many more activated T cells than other lymphoid tissues. Because SIV/HIV-1 can replicate optimally in activated T cells, the mesenteric lymph nodes might release the largest numbers of infectious virus.

After the peak of viraemia, the titre of infectious virus in the lymphoid tissues decreased significantly. Around this time, it is generally recognized that adaptive immunity is induced in the host. Therefore, the induction of such acquired immunity might also result in the suppression of virus replication in the lymphoid tissues. Moreover, $CD4^+$ T cells, which are the main target and source of amplification of the virus (Dalgleish *et al.*, 1984; Klatzmann *et al.*, 1984; Sattentau *et al.*, 1988), were depleted in the lymphoid tissues by this time, thus resulting in the low level of virus production there. In contrast, significant proviral DNA remained in the lymphoid tissues after the peak of viraemia. The identity of the cells holding this proviral DNA was not clear, but they might represent a reservoir pool of virus until the development of AIDS.

In the intestinal tract, infectious virus was detected, but the virus load was much lower than in the lymphoid tissues. This is surprising because it was expected that the intestinal tract would have as many activated lymphocytes as the mesenteric lymph node and the virus replicates efficiently in those cells. Some reasons for the low titre of infectious virus in the intestinal tract were considered. Firstly, the sample of intestinal tract, which was separated as iEL and LPL, contains various types of cells and the percentage of $CD4^+$ T cells there was much lower than in samples of lymphoid tissues, thus giving rise to a lower level of virus production in the intestinal tract. In addition, there is a possibility that the intestinal tract has a strong immunity. Following virus infection, the components of innate immunity might respond rapidly and provide time for the subsequent development of adaptive immunity. Natural killer (NK) cells, which are a critical component of innate immunity to virus infection, were reported to mediate suppression of HIV-1 replication by producing CC chemokines or causing cytotoxicity against HIV-1-infected cells (Baum *et al.*, 1996; Fehniger *et al.*, 1998; Kottilil *et al.*, 2003; Levy, 2001; Oliva *et al.*, 1998). In the monkeys used in this study, NK activity using K562 target cells was measured in PBMCs, intestinal tract and inguinal and mesenteric lymph nodes (K. Ibuki, N. Saito, Y. Enose, A. Miyake, H. Suzuki, R. Horiuchi, T. Miura & M. Hayami, unpublished data). Among these tissues, NK activity was much higher in the intestinal tract of both normal and infected monkeys. This result raises the possibility that NK activity in the intestinal tract contributed to the suppression of virus replication in the present study.

In the lymphoid tissues, levels of $CD4^+$ T cells decreased significantly from day 6 p.i. In contrast, in the intestinal tract, $CD4^+$ T cells remained at the same level as in uninfected normal controls until 13 days p.i. These results clearly correlated with the extent of virus replication in the lymphoid tissues and intestinal tract. However, $CD4^+$ T cells in the intestinal tract were finally depleted by 27 days p.i. In previous studies, it was reported that the target tissues or organs of the virus differed when using CXCR4 or CCR5 as

co-receptors of virus entry (Harouse *et al.*, 1999; Reyes *et al.*, 2004). In the early phase of infection, CXCR4-utilizing SHIV causes rapid depletion of $CD4^+$ T cells in the peripheral blood, but not in the intestinal tissues, whereas CCR5-utilizing SHIV causes rapid depletion of $CD4^+$ T cells in the intestinal tissues, but not in the peripheral blood. Recent studies using SIV-infected monkeys showed a profound and selective loss of memory $CD4^+$ $CCR5^+$ T cells in the intestinal tract in the early phase of infection (Brenchley *et al.*, 2004; Mehandru *et al.*, 2004; Mattapallil *et al.*, 2005; Li *et al.*, 2005). Moreover, some HIV-1-carrier studies demonstrated that a significant and preferential depletion of mucosal $CD4^+$ T cells that express CCR5 occurs compared with peripheral blood or lymphoid tissues (Veazey *et al.*, 2000a, b; Centlivre *et al.*, 2005). SIV and most primary isolated HIV-1 utilize CCR5 as co-receptor for entry, and target tissues of dual-tropic virus using both CXCR4 and CCR5 were unknown. In this study, it was shown that SHIV-C2/1 using both CXCR4 and CCR5 as co-receptors caused rapid $CD4^+$ T-cell depletion in both peripheral blood and the intestinal tract.

Among the tissues examined, the thymus and intestinal tract had a large percentage of CD4CD8 DP T cells. Both tissues have been reported as sites of maturation of lymphocytes (Haynes *et al.*, 1990; Lundqvist *et al.*, 1995) and CD4CD8 DP T cells have been proposed to be immature T cells. A previous study reported that CD4CD8 DP T cells in the thymus were susceptible to HIV-1 infection (Schnittman *et al.*, 1990). Moreover, CD4 SP and CD4CD8 DP T cells were found to decrease at the same time during acute SIV infection in rhesus macaques in the thymus (Rosenzweig *et al.*, 2000) and intestinal tract (Mattapallil *et al.*, 2000; Smit-McBride *et al.*, 1998). In this study, however, CD4CD8 DP T cells started to decrease earlier than mature CD4 SP T cells in both the thymus and intestinal tract, suggesting that the resultant effect of virus infection is different between the mature and immature T cells in each tissue. CD4CD8 DP T cells were observed to decrease in both tissues before virus replication. This shows that the virus may indirectly kill CD4CD8 DP T cells. Moreover, $CD3^-$ CD4CD8 DP cells, which are precursors of $CD3^+$ CD4CD8 DP cells (Hori *et al.*, 1991), were also depleted in the thymus after the peak of viraemia. Further studies of the pathogenesis of virus infection in immature T cells of the thymus and intestinal tract may lead to better understanding of the mechanisms of $CD4^+$ cell depletion in HIV-1-infected humans.

ACKNOWLEDGEMENTS

We thank James Raymond for the editing of this manuscript. This work was supported by a Health Sciences Research Grant from the Ministry of Health, Labour and Welfare, Japan and a Grant-in-Aid for Scientific Research from the Ministry of Education and Science, Japan. A. M. is a recipient of a Research Resident Fellowship for junior researchers of the Japanese Foundation for AIDS Prevention.

REFERENCES

Baum, L. L., Cassutt, K. J., Knigge, K. & 7 other authors (1996). HIV-1 gp120-specific antibody-dependent cell-mediated cytotoxicity correlates with rate of disease progression. *J Immunol* **157**, 2168–2173.

Brenchley, J. M., Schacker, T. W., Ruff, L. E. & 8 other authors (2004). $CD4^+$ T cell depletion during all stages of HIV disease occurs predominantly in the gastrointestinal tract. *J Exp Med* **200**, 749–759.

Cantó-Nogués, C., Jones, S., Sangster, R. & 8 other authors (2001). *In situ* hybridization and immunolabelling study of the early replication of simian immunodeficiency virus (SIVmacJ5) *in vivo*. *J Gen Virol* **82**, 2225–2234.

Centlivre, M., Sommer, P., Michel, M. & 8 other authors (2005). HIV-1 clade promoters strongly influence spatial and temporal dynamics of viral replication in vivo. *J Clin Invest* **115**, 348–358.

Chun, T.-W., Carruth, L., Finzi, D. & 12 other authors (1997). Quantification of latent tissue reservoirs and total body viral load in HIV-1 infection. *Nature* **387**, 183–188.

Clapham, P. R., Weiss, R. A., Dalgleish, A. G., Exley, M., Whitby, D. & Hogg, N. (1987). Human immunodeficiency virus infection of monocytic and T-lymphocytic cells: receptor modulation and differentiation induced by phorbol ester. *Virology* **158**, 44–51.

Couëdel-Courteille, A., Butor, C., Juillard, V., Guillet, J.-G. & Venet, A. (1999). Dissemination of SIV after rectal infection preferentially involves paracolic germinal centers. *Virology* **260**, 277–294.

Couëdel-Courteille, A., Prétet, J.-L., Barget, N., Jacques, S., Petitprez, K., Tulliez, M., Guillet, J.-G., Venet, A. & Butor, C. (2003). Delayed viral replication and $CD4^+$ T cell depletion in the rectosigmoid mucosa of macaques during primary rectal SIV infection. *Virology* **316**, 290–301.

Dalgleish, A. G., Beverley, P. C., Clapham, P. R., Crawford, D. H., Greaves, M. F. & Weiss, R. A. (1984). The CD4 (T4) antigen is an essential component of the receptor for the AIDS retrovirus. *Nature* **312**, 763–767.

Fauci, A. S. (1996). Host factors in the pathogenesis of HIV disease. *Antibiot Chemother* **48**, 4–12.

Fehniger, T. A., Herbein, G., Yu, H., Para, M. I., Bernstein, Z. P., O'Brien, W. A. & Caligiuri, M. A. (1998). Natural killer cells from $HIV\text{-}1^+$ patients produce C-C chemokines and inhibit HIV-1 infection. *J Immunol* **161**, 6433–6438.

Harouse, J. M., Gettie, A., Tan, R. C. H., Blanchard, J. & Cheng-Mayer, C. (1999). Distinct pathogenic sequela in rhesus macaques infected with CCR5 or CXCR4 utilizing SHIVs. *Science* **284**, 816–819.

Haynes, B. F., Denning, S. M., Le, P. T. & Singer, K. H. (1990). Human intrathymic T cell differentiation. *Semin Immunol* **2**, 67–77.

Hirsch, V. M., Sharkey, M. E., Brown, C. R. & 8 other authors (1998). Vpx is required for dissemination and pathogenesis of SIV_{SM} PBj: evidence of macrophage-dependent viral amplification. *Nat Med* **4**, 1401–1408.

Hori, T., Cupp, J., Wrighton, N., Lee, F. & Spits, H. (1991). Identification of a novel human thymocyte subset with a phenotype of CD3− CD4+ CD8 alpha+beta-1. Possible progeny of the CD3− CD4− CD8− subset. *J Immunol* **146**, 4078–4084.

Hu, J., Gardner, M. B. & Miller, C. J. (2000). Simian immunodeficiency virus rapidly penetrates the cervicovaginal mucosa after intravaginal inoculation and infects intraepithelial dendritic cells. *J Virol* **74**, 6087–6095.

Joag, S. V., Adany, I., Li, Z., Foresman, L., Pinson, D. M., Wang, C., Stephens, E. B., Raghavan, R. & Narayan, O. (1997). Animal model of mucosally transmitted human immunodeficiency virus type 1

disease: intravaginal and oral deposition of simian/human immunodeficiency virus in macaques results in systemic infection, elimination of $CD4^+$ T cells, and AIDS. *J Virol* **71**, 4016–4023.

Kato, S., Hiraishi, Y., Nishimura, N., Sugita, T., Tomihama, M. & Takano, T. (1998). A plaque hybridization assay for quantifying and cloning infectious human immunodeficiency virus type 1 virions. *J Virol Methods* **72**, 1–7.

Klatzmann, D., Champagne, E., Chamaret, S., Gruest, J., Guetard, D., Hercend, T., Gluckman, J. C. & Montagnier, L. (1984). T-lymphocyte T4 molecule behaves as the receptor for human retrovirus LAV. *Nature* **312**, 767–768.

Kottilil, S., Chun, T.-W., Moir, S., Liu, S., McLaughlin, M., Hallahan, C. W., Maldarelli, F., Corey, L. & Fauci, A. S. (2003). Innate immunity in human immunodeficiency virus infection: effect of viremia on natural killer cell function. *J Infect Dis* **187**, 1038–1045.

Levy, J. A. (2001). The importance of the innate immune system in controlling HIV infection and disease. *Trends Immunol* **22**, 312–316.

Li, Q., Duan, L., Estes, J. D. & 7 other authors (2005). Peak SIV replication in resting memory $CD4^+$ T cells depletes gut lamina propria $CD4^+$ T cells. *Nature* **434**, 1148–1152.

Lu, Y., Pauza, C. D., Lu, X., Montefiori, D. C. & Miller, C. J. (1998). Rhesus macaques that become systemically infected with pathogenic SHIV 89.6-PD after intravenous, rectal, or vaginal inoculation and fail to make an antiviral antibody response rapidly develop AIDS. *J Acquir Immune Defic Syndr Hum Retrovirol* **19**, 6–18.

Lundqvist, C., Baranov, V., Hammarstrom, S., Athlin, L. & Hammarstrom, M. L. (1995). Intra-epithelial lymphocytes. Evidence for regional specialization and extrathymic T cell maturation in the human gut epithelium. *Int Immunol* **7**, 1473–1487.

Mattapallil, J. J., Reay, E. & Dandekar, S. (2000). An early expansion of $CD8\alpha\beta$ T cells, but depletion of resident $CD8\alpha\alpha$ T cells, occurs in the intestinal epithelium during primary simian immunodeficiency virus infection. *AIDS* **14**, 637–646.

Mattapallil, J. J., Douek, D. C., Hill, B., Nishimura, Y., Martin, M. & Roederer, M. (2005). Massive infection and loss of memory $CD4^+$ T cells in multiple tissues during acute SIV infection. *Nature* **434**, 1093–1097.

Mehandru, S., Poles, M. A., Tenner-Racz, K., Horowitz, A., Hurley, A., Hogan, C., Boden, D., Racz, P. & Markowitz, M. (2004). Primary HIV-1 infection is associated with preferential depletion of $CD4^+$ T lymphocytes from effector sites in the gastrointestinal tract. *J Exp Med* **200**, 761–770.

Mellors, J. W., Kingsley, L. A., Rinaldo, C. R., Jr, Todd, J. A., Hoo, B. S., Kokka, R. P. & Gupta, P. (1995). Quantitation of HIV-1 RNA in plasma predicts outcome after seroconversion. *Ann Intern Med* **122**, 573–579.

Miller, C. J., Li, Q., Abel, K. & 12 other authors (2005). Propagation and dissemination of infection after vaginal transmission of simian immunodeficiency virus. *J Virol* **79**, 9217–9227.

Milush, J. M., Kosub, D., Marthas, M., Schmidt, K., Scott, F., Wozniakowski, A., Brown, C., Westmoreland, S. & Sodora, D. L. (2004). Rapid dissemination of SIV following oral inoculation. *AIDS* **18**, 2371–2380.

Miyake, A., Enose, Y., Ohkura, S., Suzuki, H., Kuwata, T., Shimada, T., Kato, S., Narayan, O. & Hayami, M. (2004). The quantity and diversity of infectious viruses in various tissues of SHIV-infected monkeys at the early and AIDS stages. *Arch Virol* **149**, 943–955.

Oliva, A., Kinter, A. L., Vaccarezza, M. & 10 other authors (1998). Natural killer cells from human immunodeficiency virus (HIV)-infected individuals are an important source of CC-chemokines and suppress HIV-1 entry and replication in vitro. *J Clin Invest* **102**, 223–231.

O'Neil, S. P., Mossman, S. P., Maul, D. H. & Hoover, E. A. (1999). In vivo cell and tissue tropism of SIVsmmPBj14-bcl.3. *AIDS Res Hum Retroviruses* **15**, 203–215.

Reyes, R. A., Canfield, D. R., Esser, U., Adamson, L. A., Brown, C. R., Cheng-Mayer, C., Gardner, M. B., Harouse, J. M. & Luciw, P. A. (2004). Induction of simian AIDS in infant rhesus macaques infected with CCR5- or CXCR4-utilizing simian-human immunodeficiency viruses is associated with distinct lesions of the thymus. *J Virol* **78**, 2121–2130.

Rosenzweig, M., Connole, M., Forand-Barabasz, A., Tremblay, M.-P., Johnson, R. P. & Lackner, A. A. (2000). Mechanisms associated with thymocyte apoptosis induced by simian immunodeficiency virus. *J Immunol* **165**, 3461–3468.

Sattentau, Q. J., Clapham, P. R., Weiss, R. A., Beverley, P. C., Montagnier, L., Alhalabi, M. F., Gluckmann, J. C. & Klatzmann, D. (1988). The human and simian immunodeficiency viruses HIV-1, HIV-2 and SIV interact with similar epitopes on their cellular receptor, the CD4 molecule. *AIDS* **2**, 101–105.

Schacker, T., Collier, A. C., Hughes, J., Shea, T. & Corey, L. (1996). Clinical and epidemiologic features of primary HIV infection. *Ann Intern Med* **125**, 257–264.

Schnittman, S. M., Denning, S. M., Greenhouse, J. J., Justement, J. S., Baseler, M., Kurtzberg, J., Haynes, B. F. & Fauci, A. S. (1990). Evidence for susceptibility of intrathymic T-cell precursors and their progeny carrying T-cell antigen receptor phenotypes $TCR\alpha\beta^+$ and $TCR\gamma\delta^+$ to human immunodeficiency virus infection: a mechanism for $CD4^+$ (T4) lymphocyte depletion. *Proc Natl Acad Sci U S A* **87**, 7727–7731.

Sei, S., Kleiner, D. E., Kopp, J. B., Chandra, R., Klotman, P. E., Yarchoan, R., Pizzo, P. A. & Mitsuya, H. (1994). Quantitative analysis of viral burden in tissues from adults and children with symptomatic human immunodeficiency virus type 1 infection assessed by polymerase chain reaction. *J Infect Dis* **170**, 325–333.

Shinohara, K., Sakai, K., Ando, S. & 10 other authors (1999). A highly pathogenic simian/human immunodeficiency virus with genetic changes in cynomolgus monkey. *J Gen Virol* **80**, 1231–1240.

Smit-McBride, Z., Mattapallil, J. J., McChesney, M., Ferrick, D. & Dandekar, S. (1998). Gastrointestinal T lymphocytes retain high potential for cytokine responses but have severe $CD4^+$ T-cell depletion at all stages of simian immunodeficiency virus infection compared to peripheral lymphocytes. *J Virol* **72**, 6646–6656.

Spira, A. I., Marx, P. A., Patterson, B. K., Mahoney, J., Koup, R. A., Wolinsky, S. M. & Ho, D. D. (1996). Cellular targets of infection and route of viral dissemination after an intravaginal inoculation of simian immunodeficiency virus into rhesus macaques. *J Exp Med* **183**, 215–225.

Stahl-Hennig, C., Steinman, R. M., Tenner-Racz, K. & 7 other authors (1999). Rapid infection of oral mucosal-associated lymphoid tissue with simian immunodeficiency virus. *Science* **285**, 1261–1265.

Suryanarayana, K., Wiltrout, T. A., Vasquez, G. M., Hirsch, V. M. & Lifson, J. D. (1998). Plasma SIV RNA viral load determination by real-time quantification of product generation in reverse transcriptase-polymerase chain reaction. *AIDS Res Hum Retroviruses* **14**, 183–189.

Veazey, R. S., Rosenzweig, M., Shvetz, D. E., Pauley, D. R., DeMaria, M., Chalifoux, L. V., Johnson, R. P. & Lackner, A. A. (1997). Characterization of gut-associated lymphoid tissue (GALT) of normal rhesus macaques. *Clin Immunol Immunopathol* **82**, 230–242.

Veazey, R. S., DeMaria, M., Chalifoux, L. V. & 7 other authors (1998). Gastrointestinal tract as a major site of $CD4^+$ T cell depletion and viral replication in SIV infection. *Science* **280**, 427–431.

Veazey, R. S., Mansfield, K. G., Tham, I. C., Carville, A. C., Shvetz, D. E., Forand, A. E. & Lackner, A. A. (2000a). Dynamics of CCR5

expression by $CD4^+$ T cells in lymphoid tissues during simian immunodeficiency virus infection. *J Virol* **74**, 11001–11007.

Veazey, R. S., Tham, I. C., Mansfield, K. G., DeMaria, M., Forand, A. E., Shvetz, D. E., Chalifoux, L. V., Sehgal, P. K. & Lackner, A. A. (2000b). Identifying the target cell in primary simian immunodeficiency virus (SIV) infection: highly activated memory $CD4^+$ T cells are rapidly eliminated in early SIV infection in vivo. *J Virol* **74**, 57–64.

Zhang, Z.-Q., Schuler, T., Zupancic, M. & 21 other authors (1999). Sexual transmission and propagation of SIV and HIV in resting and activated $CD4^+$ T cells. *Science* **286**, 1353–1357.

Leukemia (2006) 20, 800–806

www.nature.com/leu

ORIGINAL ARTICLE

DHMEQ, a new NF-κB inhibitor, induces apoptosis and enhances fludarabine effects on chronic lymphocytic leukemia cells

R Horie[1,2,6], M Watanabe[1,6], T Okamura[3], M Taira[1], M Shoda[2], T Motoji[3], A Utsunomiya[4], T Watanabe[2], M Higashihara[1] and K Umezawa[5]

[1]*Department of Hematology, School of Medicine, Kitasato University, Sagamihara, Kanagawa, Japan;* [2]*Laboratory of Tumor Cell Biology, Department of Medical Genome Sciences, Graduate School of Frontier Sciences, The University of Tokyo, Minato-ku, Tokyo, Japan;* [3]*Department of Hematology, Tokyo Women's Medical University, Shinjyuku-Ku, Tokyo, Japan;* [4]*Department of Hematology, Imamura Branch Hospital, Kagoshima, Japan and* [5]*Department of Applied Chemistry, Faculty of Science and Technology, Keio University, Yokohama, Kanagawa, Japan*

Chronic lymphocytic leukemia (CLL) is a low-grade lymphoid malignancy incurable with conventional modalities of chemotherapy. Strong and constitutive nuclear factor kappa B (NF-κB) activation is a characteristic of CLL cells. We examined the effects of a new NF-κB inhibitor, dehydroxymethylepoxyquinomicin (DHMEQ), on CLL cells. Dehydroxymethylepoxyquinomicin completely abrogated constitutive NF-κB activity and induced apoptosis of CLL cells. Apoptosis induced by DHMEQ was accompanied by downregulation of NF-κB-dependent antiapoptotic genes: c-IAP, Bfl-1, Bcl-X_L and c-FLIP. Dehydroxymethylepoxyquinomicin also inhibited NF-κB induced by CD40 and enhanced fludarabine-mediated apoptosis of CLL cells. Results of this study suggest that inhibition of constitutive and inducible NF-κB by DHMEQ in combination with fludarabine is a promising strategy for the treatment of CLL.
Leukemia (2006) **20**, 800–806. doi:10.1038/sj.leu.2404167; published online 9 March 2006
Keywords: CLL; NF-κB; apoptosis; DHMEQ; fludarabine

Introduction

Chronic lymphocytic leukemia (CLL) is a low-grade B-cell malignancy predominantly affecting adults over the age of 50 years. The disease course is variable but remains incurable despite development of nucleoside analogues such as fludarabine and 2-chlorodeoxyadenosine (cladribine).[1] Development of a new treatment option based on the biological basis of CLL cells is needed to improve the prognosis of CLL. Most chemotherapeutic agents target the process of DNA replication and division of cells, therefore are more effective in tumor cells having high proliferation activity. These agents are not well suited for the treatment of CLL that shows not proliferation but instead an accumulation of cells through resistance to apoptosis.[2]

Recently, treatment strategies to target molecules that support the maintenance and growth of the tumor cells have been pursued.[3] Molecular target therapy increases the specificity of the agent to tumor cells, thereby minimizes undesirable toxicity to normal cells and provides an opportunity to cure malignancies incurable by conventional chemotherapy.[4,5]

It is important for development of a new treatment strategy of CLL to clarify a common biological basis for deregulated apoptosis and to develop specific agents that target the required molecule(s). Despite the diversity in clinical manifestations of CLL, strong and constitutive nuclear factor kappa B (NF-κB) activity is reported to be a common characteristic of CLL cells.[6] NF-κB activation has been connected with control of apoptosis.[7,8] This background suggests that in CLL cells, constitutively active NF-κB antagonizes apoptotic pathways leading to inappropriate survival of tumor cells. Recent studies using antibody against CD40 ligand (CD40L), which inhibits CD40 signaling, and a proteasome inhibitor support this hypothesis.[6,9,10] If so, targeting the NF-κB pathway and inhibition of NF-κB activity is a logical strategy to treat CLL.

Dehydroxymethylepoxyquinomicin (DHMEQ) is a new NF-κB inhibitor that is a 5-dehydroxymethyl derivative of a novel compound epoxyquinomicin C.[11] We showed that DHMEQ inhibits nuclear translocation of NF-κB.[12]

In the present study, using a new NF-κB inhibitor DHMEQ, we present data that indicate that constitutive NF-κB activation supports survival of CLL cells by induction of antiapoptotic genes. Dehydroxymethylepoxyquinomicin inhibited NF-κB activity induced by CD40 and enhanced fludarabine-mediated apoptosis of CLL cells, suggesting that inhibition of constitutive and inducible NF-κB by DHMEQ in combination with fludarabine is a promising strategy for the future treatment of CLL.

Materials and methods

Patients

All patients ($n=15$) were previously diagnosed as having B-cell CLL according to established clinical and laboratory criteria.[13] Patients were either untreated ($n=7$) or had received cytoreductive chemotherapy before investigation ($n=8$). Relevant clinical and laboratory data of the patients are included in Table 1.

Separation procedures and culture

Peripheral blood mononuclear cells (PBMC) were isolated from heparinized blood samples obtained after informed consent using gradient centrifugation with Lymphoprep (AXIS SHIELD PoC AS, Oslo, Norway). Chronic lymphocytic leukemia cells were purified using a Dynal B-cell-negative isolation kit (Dynal Biotech, Oslo, Norway). This method produced more than 95% pure population of CLL cells expressing both CD19 and CD5 (mean 97.8%), as determined by flow cytometry using antibodies anti-CD19/FITC and anti-CD5/PE (Dako, Kyoto,

Correspondence: Dr R Horie, Department of Hematology, School of Medicine, Kitasato University, 1-15-1 Kitasato, Sagamihara, Kanagawa 228-8555, Japan.
E-mail: rhorie@med.kitasato-u.ac.jp
[6]These authors contributed equally to this work.
Received 20 August 2005; revised 27 January 2006; accepted 30 January 2006; published online 9 March 2006

Table 1 Clinical data of the patients studied

Case #	Age (years)	Sex	WBC	Hb	Plt	Stage (Binet/Rai)	Therapy
1	89	M	41.2	11.6	14.7	A/0	None
2	58	M	33.3	14.2	13.8	A/0	None
3	67	M	20.0	12.7	13.7	A/0	None
4	88	M	14.8	12.0	10.8	A/0	None
5	67	M	7.8	9.5	16.1	C/IV	Fludara+Pred
6	79	M	71.2	12.4	9.5	C/IV	None
7	57	M	53.5	11.8	16.1	A/II	Fludara
8	83	F	26.5	15.2	11.6	A/0	None
9	62	M	48.7	7.6	2.7	C/IV	Fludara
10	72	M	23.1	14.3	10.7	A/0	None
11	72	F	74.5	9.2	10.2	C/III	CVP
12	70	F	12.8	8.4	1.7	C/IV	Fludara
13	72	F	202.5	6.9	1.6	C/IV	Fludara
14	89	M	133.9	7.6	5.9	C/IV	Fludara
15	75	M	90.8	11.2	8.7	C/IV	Cyclo

Abbreviations: CVP, cyclophosphamide, vincristine, prednisolone; Cyclo, cyclophosphamide; Fludara, fludarabine; Hb, hemoglobin (g/dl); Plt, platelet count ($\times 10^4/\mu l$); WBC, white blood cell count ($\times 10^3/\mu l$).

Japan). We purified normal B cells using the same method, which produced more than 90% pure population of B cells (mean 92.7%), assessed by flow cytometry staining with anti-CD19/FITC antibody (Dako, Kyoto, Japan). Cells were cultured at 37°C with 5% CO_2 in RPMI 1640 supplemented with 20% fetal bovine serum and antibiotics.

Chemicals

Dehydroxymethylepoxyquinomicin is an NF-κB inhibitor that blocks nuclear translocation of NF-κB.[11,12] An active metabolite of fludarabine, 2-fluoroadenine-9-β-D-arabinofuranoside (F-ara-A), was purchased from Sigma (St Louis, MO, USA). Dehydroxymethylepoxyquinomicin and F-ara-A were dissolved with dimethylsulfoxide (DMSO) and used for experiments at indicated concentrations. Bisbenzimide H 33342 fluorochrome (Hoechst 33342) and caspase-3 inhibitor Z-Asp-Glu-Val-Asp-(DEVD)-FMK were purchased from Calbiochem (Bad Soden, Germany).

Electrophoretic mobility shift analysis

Electrophoretic mobility shift analysis (EMSA) was carried out according to the methods described previously.[14] Double-stranded oligonucleotide probes containing the mouse immunoglobulin-κ light-chain NF-κB consensus site were purchased from Promega (Madison, WI, USA). Antibodies used for supershift assays were as follows: NF-κB p50 (C-19) goat polyclonal antibody, NF-κB p65 (C-20) and RelB (C-19) rabbit polyclonal antibody and mouse monoclonal antibodies for c-Rel (B-6) and NF-κB p52 (C-5) (all from Santa Cruz Biotechnology Inc., Santa Cruz, CA, USA).

Cell viability assay

Effects of DHMEQ on cell viability were assayed by color reaction with 3-(4,5-dimethylthiazol-2-yl)-2,5-diphenyl tetrazolium bromide (MTT assay) as described previously.[15] After incubation with DHMEQ at the indicated concentrations and time points, 2×10^5 cells treated by MTT solution were measured by a microplate reader (Bio-Rad, Richmond, CA, USA) at a reference wavelength of 570 nm and test wavelength of 450 nm. The cell viability was expressed as a percentage of the DMSO-treated control samples.

Apoptosis and analysis of caspase activity

To quantify apoptosis, cells were labeled with FITC-conjugated Annexin V (BD Biosciences, Palo Alto, CA, USA) followed by flow cytometric analysis. For analysis of morphological changes of nuclei, cells were stained by 10 μM Hoechst 33342, and photographed through a UV filter. Detection of cleaved caspase 3 was performed by immunohistochemistry. Antibodies used in these experiments were as follows: rabbit polyclonal antibody for cleaved caspase 3 (Asp175) (Cell Signaling, Beverly, MA, USA) and for glyceraldehyde phosphate dehydrogenase (FL335) (Santa Cruz Biotechnology Inc.). Mouse monoclonal antibody for Fas (CH-11) (Medical and Biological Laboratories Co., Ltd, Nagoya, Japan) was used for stimulation of Fas.

Real-time PCR analysis

Total RNA from isolated CLL cells was extracted using ISOGEN (Nippon Gene Co., Tokyo, Japan) according to the manufacturer's instructions. Single-stranded cDNA was synthesized using TaqMan Reverse Transcription Reagents (Applied Biosystems, Norwalk, CT, USA). The primers for Bcl-X_L; Hs00236329_m1 (BCL2L1) c-IAP; Hs00154109_m1 (BIRC3), Bfl-1; Hs00187845_m1 (BCL2A1) and c-FLIP; Hs00153439_m1 (CFLAR) were purchased from Applied Biosystems (Tokyo, Japan). The conditions of real-time PCR were as follows: 1 μl of cDNA was added to 25 μl of TaqMan Gene Expression Assays and made up to a total volume of 50 μl with distilled water for each reaction. Thermal cycler conditions were 2 min at 50°C, 10 min at 95°C and then 40 cycles of 15 s at 95°C followed by 1 min at 60°C. Results were collected and analyzed using an ABI PRISM 7000 sequence detection system (Applied Biosystems).

Statistical analysis

Differences between mean values were assessed by two-tailed *t*-test. A *P*-value <0.05 was considered to be statistically significant.

Results

Effects of DHMEQ on constitutive NF-κB activity in primary CLL cells

First we examined the effect of DHMEQ on constitutive NF-κB activity and its time course in CLL cells ($n=5$; #1, 2, 6, 7 and 14) by EMSA. As described previously, high NF-κB DNA binding activity was detected in nuclear extracts from CLL cells.[16] Treatment with 10 μg/ml of DHMEQ almost completely abrogated NF-κB DNA binding activity within 2 h. DNA binding activity of untreated CLL cells served as controls. Representative results (#7 and 14) are shown in Figure 1a. Supershift analysis of CLL cells ($n=5$; #1, 2, 6, 7 and 15) showed that NF-κB DNA binding activity consists of p50 homodimer (lower band) and p50/p65 heterodimer (upper band). Representative results (#2 and 15) are shown in Figure 1b. We next examined the effect of DHMEQ on constitutive NF-κB activity in all CLL cases studied ($n=15$). Treatment with 10 μg/ml of DHMEQ completely blocked NF-κB DNA binding activity in all cases. The results of 10 cases are shown in Figure 1c.

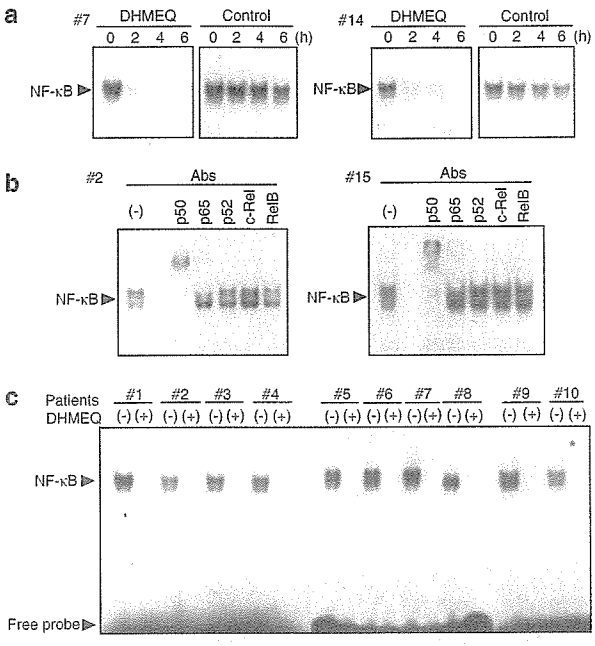

Figure 1 Inhibition of constitutive nuclear factor kappa B (NF-κB) activity in CLL cells by dehydroxymethylepoxyquinomicin (DHMEQ). (**a**) Time-course studies of NF-κB inhibition by DHMEQ. Chronic lymphocytic leukemia cells were treated with 10 μg/ml of DHMEQ for the indicated hours. Nuclear extracts (2 μg) were examined for NF-κB binding activity by electrophoretic mobility shift analysis (EMSA) with a radiolabeled NF-κB-specific probe. (**b**) NF-κB subcomponent analysis in CLL cells. Subcomponents of NF-κB constitutively activated in CLL cells were determined by supershift analysis. Nuclear extracts (2 μg) of cells untreated with DHMEQ were subjected to supershift analysis with antibodies specific for NF-κB p50, p65, p52, c-Rel and RelB. (**c**) Inhibition of constitutive NF-κB binding activity in CLL cells. Chronic lymphocytic leukemia cells were treated with (+) or without (−) 10 μg/ml of DHMEQ for 3 h. Nuclear extracts (2 μg) were examined for NF-κB binding activity by EMSA with a radiolabeled NF-κB-specific probe. The position of shifted bands corresponding to NF-κB and free probes are indicated on the left.

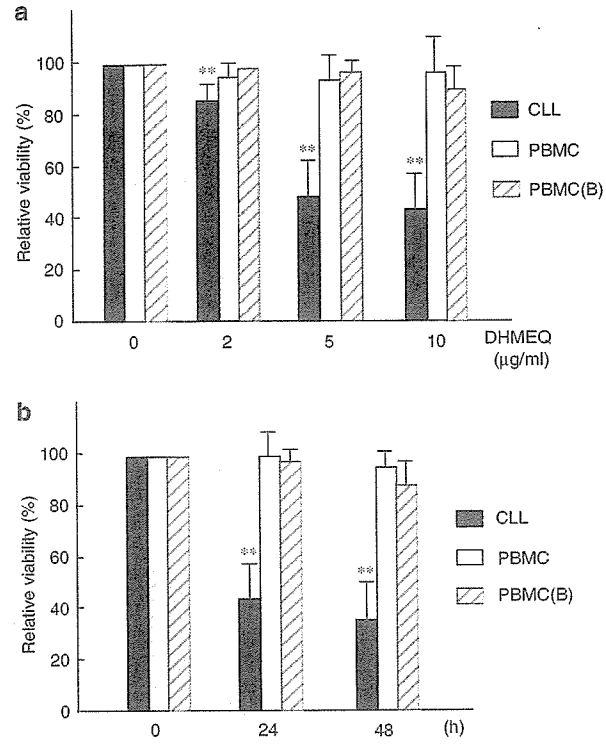

Figure 2 Dehydroxymethylepoxyquinomicin (DHMEQ) reduces viability of chronic lymphocytic leukemia (CLL) cells. Reduction of viability of CLL cells treated with DHMEQ. Chronic lymphocytic leukemia cells, peripheral blood mononuclear cells and purified B cells were treated with indicated concentrations of DHMEQ for 48 h (**a**) or were treated for the indicated hours with 10 μg/ml of DHMEQ (**b**). Cell viabilities were determined by MTT assay. For each case, experiments were carried out in triplicate. The data are means ± s.d. of indicated cases. $^{**}P<0.01$.

DHMEQ selectively induces apoptosis of CLL cells

To evaluate an effect of constitutively active NF-κB on the survival of CLL cells, we treated CLL cells ($n=15$) by DHMEQ and examined their viability. MTT assays revealed that DHMEQ reduced the viability of all CLL cells examined in a dose (2 μg/ml, 86.2 ± 5.9%, 5 μg/ml, 48.2 ± 16.8%, 10 μg/ml, 44.3 ± 16.3%) (Figure 2a) and time (24 h, 44.3 ± 16.3%, 48 h, 33.5 ± 17.4%) (Figure 2b) dependent manner and the effects were significant at all drug concentrations and incubation times tested ($P<0.01$). The effects were not significant in control PBMC ($n=5$) and purified peripheral blood B cells ($n=3$) as shown in Figure 2a and b.

Constitutively active NF-κB has been thought to antagonize apoptotic pathways leading to inappropriate survival of tumor cells.[7,8] Thus, we examined whether DHMEQ induces apoptosis of CLL cells ($n=5$; #3, 6, 7, 10 and 11). Flow cytometric analysis showed a significant increase in the number of Annexin V-positive cells after 24 h of DHMEQ treatment compared to the untreated controls (45.6 ± 7.7 vs 5.1 ± 1.2%, $P=0.01$) (Figure 3a). The increase of Annexin V-positive cells by DHMEQ treatment was not significant in control PBMC ($n=5$) and purified peripheral blood B cells ($n=3$) as shown in Figure 3a. Fragmentation and condensation of the nuclei in CLL cells were clearly demonstrated after DHMEQ treatment by Hoechst 33342 staining, but not in PBMC or purified B cells. Representative results (#11) are shown in Figure 3b. Treatment of CLL cells by DHMEQ induced expression of the cleaved form of caspase 3, whereas pretreatment with caspase-3 inhibitor Z-Asp-Glu-Val-Asp-(DEVD)-FMK reduced expression of cleaved caspase 3. Representative results (#11) are shown in Figure 3c. Jurkat cells treated by anti-Fas antibody served as a positive control for immunostaining by cleaved caspase 3. These results indicate that DHMEQ reduces viability and induces apoptosis of CLL cells.

DHMEQ downregulates expression of antiapoptotic genes

In order to understand the molecular mechanisms of apoptosis in CLL cells after NF-κB inhibition by DHMEQ, we next examined the changes of expression level of antiapoptotic genes, Bcl-X_L, c-IAP, c-FLIP and Bfl-1, after DHMEQ treatment in CLL cells ($n=8$; #2, 3, 6, 7, 9, 11, 13 and 15) by real-time PCR. These antiapoptotic genes have been reported to be under the control of NF-κB.[7] The results shown in Figure 4 demonstrate significant reduction in the following genes: Bcl-X_L (53.4 ± 35.3% reduction, $P<0.01$), c-IAP (93.3 ± 7.4% reduc-

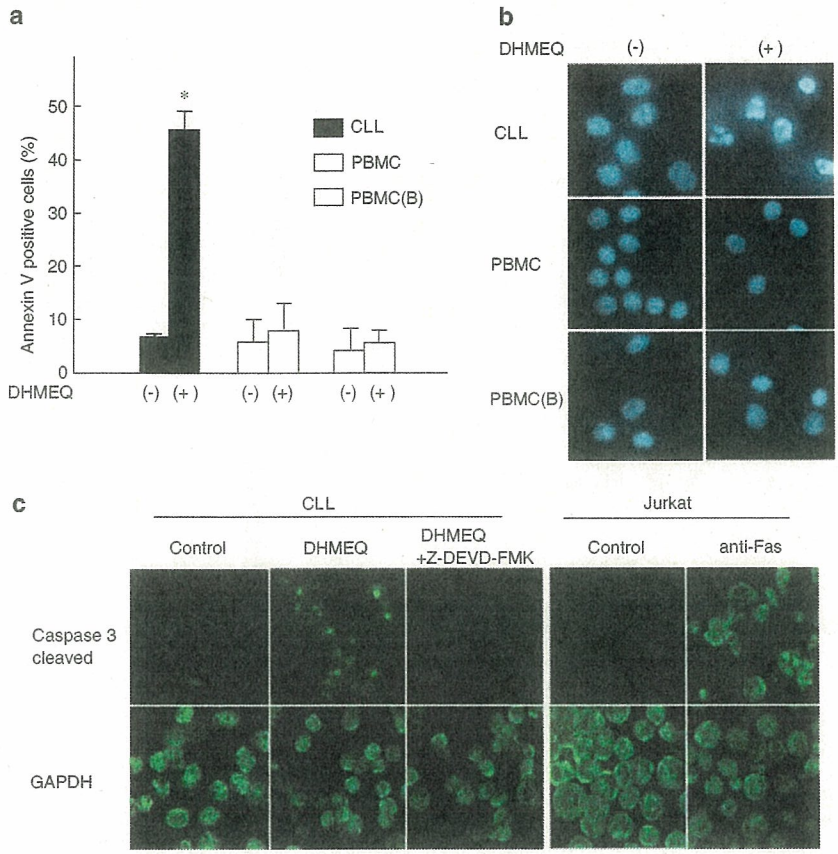

Figure 3 Dehydroxymethylepoxyquinomicin (DHMEQ) induces apoptosis of CLL cells. (**a**) Flow cytometric analysis of Annexin V-reactive cells. Chronic lymphocytic leukemia cells, peripheral blood mononuclear cells (PBMC) and purified B cells were treated with 5 μg/ml of DHMEQ for 24 h. After labeling with FITC-conjugated Annexin V, cells were analyzed by flow cytometry. For each case, experiments were carried out in triplicate. The data are means$\pm$s.d. of indicated cases. *$P<0.05$. (**b**) Nuclear fragmentation of cells treated with DHMEQ. Chronic lymphocytic leukemia cells, PBMC and purified B cells were treated with or without 10 μg/ml of DHMEQ for 24 h and stained with 10 μM Hoechst 33342. (**c**) Immunohistological detection of caspase-3 activation after DHMEQ treatment in CLL cells. Chronic lymphocytic leukemia cells were incubated with or without 5 μg/ml of DHMEQ for 24 h. For inhibition of caspase 3, 20 μM of Z-DEVD-FMK was added to the culture media 1 h before DHMEQ addition. For positive control, Jurkat cells treated with 200 ng/ml of anti-Fas antibody for 3 h were used. Cells were spun with a cytocentrifuge and stained by antibody for cleaved caspase 3 and observed by confocal microscopy. Staining of glyceraldehyde phosphate dehydrogenase (GAPDH) served as controls.

tion, $P<0.01$), c-FLIP (28.8$\pm$33.4% reduction, $P=0.04$) and Bfl-1 (93.3$\pm$8.7% reduction, $P<0.01$).

DHMEQ enhances the antitumor effect of fludarabine and inhibits CD40-mediated induction of NF-κB

We next examined whether DHMEQ could enhance the effects of fludarabine, a key chemotherapeutic agent for CLL. We first incubated CLL cells ($n=5$; #4, 6, 10, 11 and 14) with DHMEQ, F-ara-A or F-ara-A in the presence of 5 μg/ml of DHMEQ and calculated the IC_{50} (the concentration that results in 50% viability of control). F-ara-A in combination with DHMEQ significantly enhanced the IC_{50} of F-ara-A compared with F-ara-A alone (5.0$\pm$5.1 vs 11.3$\pm$5.3 μg/ml, $P=0.03$), suggesting that DHMEQ enhanced the antigrowth effect of fludarabine on CLL cells. IC_{50} of DHMEQ was 9.6$\pm$4.0 μg/ml. Representative data are shown as Figure 5a. Although experimental conditions are different compared with previous reports, IC_{50} for F-ara-A (#4; 13.2 μg/ml, #6; 12.4 μg/ml, #10; 7.8 μg/ml, #11; 12.7 μg/ml, #14; 4.0 μg/ml) indicates that cases other than #14 show potential resistance for fludarabine.[17]

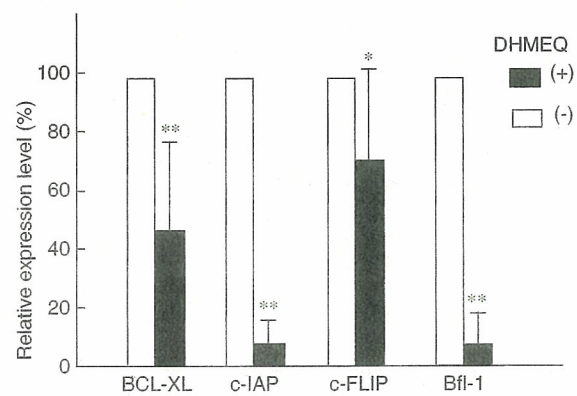

Figure 4 Effects of dehydroxymethylepoxyquinomicin (DHMEQ) on genes regulating apoptosis in chronic lymphocytic leukemia (CLL) cells. Quantification of the gene expression by real-time PCR. Chronic lymphocytic leukemia cells were treated with or without 10 μg/ml of DHMEQ for 16 h. The expressions of Bcl-X_L, c-IAP, c-FLIP and Bfl-1 were quantified by real-time PCR. For each case, experiments were carried out in triplicate. The data are means$\pm$s.d. of indicated cases. *$P<0.05$ and **$P<0.01$.

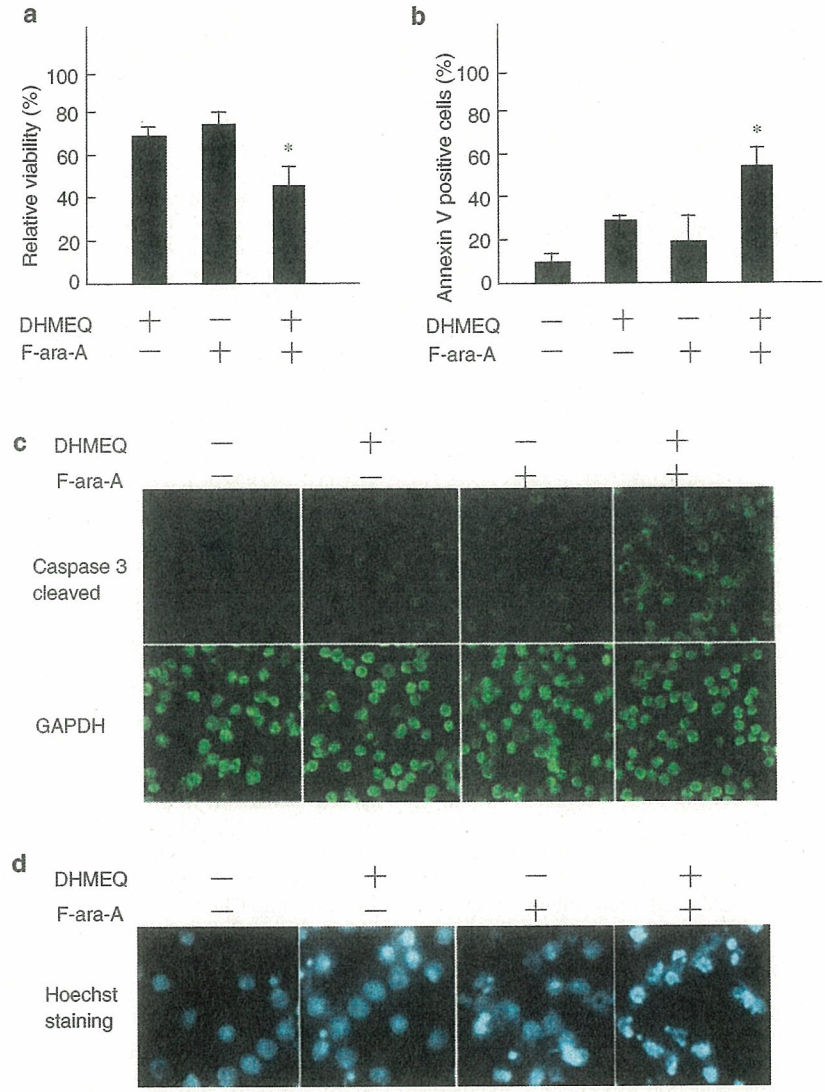

Figure 5 Dehydroxymethylepoxyquinomicin (DHMEQ) enhances antitumor effect of fludarabine in chronic lymphocytic leukemia (CLL) cells. (**a–d**) Evaluation of combined effect of DHMEQ and F-ara-A. Chronic lymphocytic leukemia cells were treated with 5 μg/ml of DHMEQ, 2 μg/ml of F-ara-A or a combination of these two agents for 24 h. (**a**) MTT assay. (**b**) Flow cytometric analysis of Annexin V-reactive cells. (**c**) Immunohistological detection of caspase 3. (**d**) Nuclear fragmentation of CLL cells detected by Hoechst 33342. In panels a and b, experiments were carried out in triplicate and the data are means $\pm$ s.d. of indicated cases. *$P<0.05$.

We further explored whether the combined effect of F-ara-A and DHMEQ results in enhanced induction of apoptosis in CLL cells. The combined treatment showed a significant increase in the number of Annexin V-positive cells when compared with F-ara-A alone (DHMEQ 30.9$\pm$2.2%; F-ara-A 19.9$\pm$12.6%; DHMEQ plus F-ara-A 53.3$\pm$10.2%, $P=0.03$) (Figure 5b). The combined treatment also showed a significant increase in the expression of the cleaved form of caspase 3 and in the fragmentation or condensation of nuclei. Representative results (#11) are shown in Figure 5c and d. These results indicate that DHMEQ enhances fludarabine-mediated apoptosis of CLL cells.

As CD40 signals were reported to play an important role in the survival of CLL cells *in vivo*, we examined the effect of DHMEQ on CD40-mediated NF-κB induction in CLL cells ($n=5$; #2, 6, 7, 9 and 13). The mean percentage of induction of NF-κB binding activity was 224.5$\pm$65.0% and significant ($P<0.01$) when the intensities of the unstimulated samples were compared with those of CD40-stimulated samples by densitometry. Dehydroxymethylepoxyquinomicin abrogated both constitutive and inducible NF-κB by CD40 activation in CLL cells. Representative results (#2, 6 and 7) are shown in Figure 6.

Discussion

Although previous work using a decoy oligonucleotide for NF-κB indicated that inhibition of NF-κB alone is not sufficient to induce apoptosis of CLL cells,[16] recent studies using proteasome inhibitors or an antibody against CD40L suggest the importance of NF-κB in the survival of CLL cells.[6,9,10] Our data clearly show that constitutive activation of NF-κB supports survival of CLL

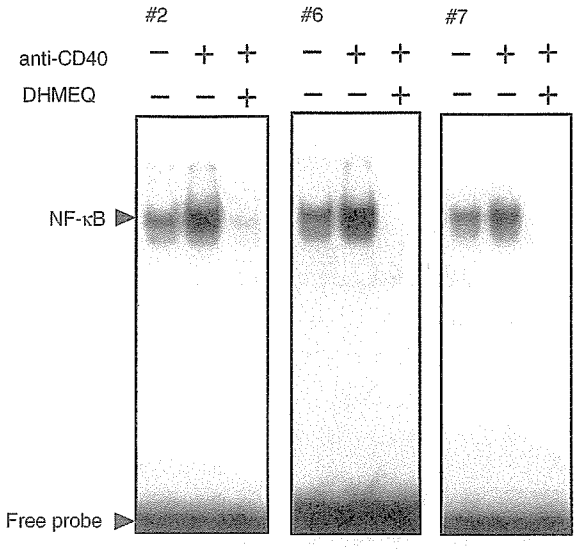

Figure 6 Dehydroxymethylepoxyquinomicin (DHMEQ) abrogates constitutive and inducible nuclear factor kappa B (NF-κB) triggered by CD40. Chronic lymphocytic leukemia (CLL) cells (1×10^6) were crosslinked by 500 ng/ml of anti-CD40 agonistic mouse antibody (Immunotech, Marseille Cedex, France) for 1 h and treated with 10 μg/ml of DHMEQ for 5 h. CLL cells crosslinked by isotype-matched IgG (Dako) served as controls. Two micrograms of nuclear extracts were examined for NF-κB binding activity by electrophoretic mobility shift analysis using a radiolabeled NF-κB probe.

cells. Discrepancies between a previous report using a decoy oligonucleotide for NF-κB and ours appear to reside in the experimental conditions and inhibitors used. Inhibition of NF-κB by DHMEQ is prompt and complete. On the other hand, inhibition of NF-κB by transduced decoy oligonucleotide appears to occur gradually. Furthermore, complete inhibition of NF-κB by the decoy oligonucleotide is difficult because of its limited transduction efficiency.

Our results also provide insights into the mechanism of DHMEQ-mediated apoptosis induction in CLL cells. Inhibition of NF-κB by DHMEQ downregulated the expression of antiapoptotic genes Bcl-X_L, c-IAP1, c-FLIP and Bfl-1, suggesting that DHMEQ-mediated apoptosis is associated with down-regulation of NF-κB-dependent genes that regulate apoptosis. Recent studies, which stress the importance of these genes on regulation of CLL cell survival, support this notion.[18,19] This also suggests that the survival of CLL is based on a balance between proapoptotic and antiapoptotic genes. Dehydroxymethylepoxy-quinomicin is thought to block antiapoptotic activity that permits the survival of CLL cells, resulting in dominance of proapoptotic activities.

The results of this study indicate that DHMEQ is a promising compound to induce NF-κB inhibition by a low molecular weight compound for the treatment of CLL. The inhibitory effect of DHMEQ on NF-κB is prompt and definitive even against the strong constitutive NF-κB activity of CLL cells. Dehydroxy-methylepoxyquinomicin treatment can induce apoptosis of CLL cells within 24–48 h. Dehydroxymethylepoxyquinomicin com-pletely abrogated NF-κB activity and reduced viability of CLL cells in all cases studied, which is independent of previous treatment. Unique properties of DHMEQ may minimize adverse effects on normal cells. Peripheral blood mononuclear cells and purified B cells are resistant to apoptosis by DHMEQ treatment. This resistance of resting cells to DHMEQ appears to be an important feature to avoid undesired effects.

In this study, we evaluated the combined effect of DHMEQ and fludarabine on survival of CLL cells. Dehydroxymethyle-poxyquinomicin enhanced the effect of fludarabine on CLL cell, but the mechanisms of action of these two agents do not overlap. Blockade of NF-κB by DHMEQ inhibits translocation of NF-κB into the nucleus and appears to induce apoptosis by downregulation of NF-κB-dependent antiapoptotic genes. On the other hand, fludarabine exerts its effects by inhibition of DNA and RNA synthesis.[20] As CLL cells reside in a quiescent state, inhibition of RNA synthesis and depletion of proteins appear to be essential for the cytotoxic action of fludarabine.[21]

Dehydroxymethylepoxyquinomicin-mediated inhibition of NF-κB may enhance the effect of fludarabine against CLL cells, especially *in vivo*. CD40 signals triggered by CLL cells themselves or by bystander normal T or B cells, expressing CD40L, drive NF-κB activity and are thought to support survival of CLL cells.[6,19] It has been reported that activation of CD40 inhibits fludarabine-induced apoptosis of CLL cells. Activation of the NF-κB pathway, which mainly involves IκB, is one mechanism of this inhibition. Activation of NF-κB triggered by CD40 is mediated by degradation of IκB and may not require protein synthesis. Thus, inhibition of protein synthesis by fludarabine through depletion of mRNA should not affect NF-κB activation by CD40.[21] In this study, we showed that DHMEQ could inhibit CD40-mediated induction of NF-κB in CLL cells. Therefore, DHMEQ appears to be a suitable compound to be used in combination with fludarabine.

In conclusion, we provided data that suggest that constitutive NF-κB activation supports survival of CLL cells and that inhibition of NF-κB by DHMEQ is a promising strategy to treat CLL. Dehydroxymethylepoxyquinomicin-mediated inhibition of NF-κB may contribute to enhance effects of fludarabine by blocking CD40-mediated NF-κB activation of CLL cells especially *in vivo*.

Acknowledgements

We thank Professor Marshall E Kadin, Harvard Medical School, for critical comments on the manuscript. This work was supported in part by Grants-in-Aid for Scientific Research from Japanese Society for Promotion of Science and Integrative Research Program of the Graduate School of Medical Sciences, Kitasato University to R Horie.

References

1 Keating MJ. Chronic lymphocytic leukemia. *Semin Oncol* 1999; **26**: 107–114.
2 Kitada S, Andersen J, Akar S, Zapata JM, Takayama S, Krajewski S *et al*. Expression of apoptosis-regulating proteins in chronic lymphocytic leukemia: correlations with *in vitro* and *in vivo* chemoresponses. *Blood* 1998; **91**: 3379–3389.
3 Griffin J. The biology of signal transduction inhibition: basic science to novel therapies. *Semin Oncol* 2001; **28**: 3–8.
4 Huang ME, Ye YC, Chen SR, Chai JR, Lu JX, Zhoa L *et al*. Use of all-trans retinoic acid in the treatment of acute promyelocytic leukemia. *Blood* 1988; **72**: 567–572.
5 Capdeville R, Silberman S, Dimitrijevic S. Imatinib: the first 3 years. *Eur J Cancer* 2002; **38** (Suppl 5): S77–S82.
6 Furman RR, Asgary Z, Mascarenhas JO, Liou HC, Schattner EJ. Modulation of NF-kappa B activity and apoptosis in chronic lymphocytic leukemia B cells. *J Immunol* 2000; **164**: 2200–2206.
7 Barkett M, Gilmore TD. Control of apoptosis by Rel/NF-kappaB transcription factors. *Oncogene* 1999; **18**: 6910–6924.

8 Guttridge DC, Albanese C, Reuther JY, Pestell RG, Baldwin Jr AS. NF-kappaB controls cell growth and differentiation through transcriptional regulation of cyclin D1. *Mol Cell Biol* 1999; **19**: 5785–5799.
9 Pahler JC, Ruiz S, Niemer I, Calvert LR, Andreeff M, Keating M *et al.* Effects of the proteasome inhibitor, bortezomib, on apoptosis in isolated lymphocytes obtained from patients with chronic lymphocytic leukemia. *Clin Cancer Res* 2003; **9**: 4570–4577.
10 Kelley TW, Alkan S, Srkalovic G, Hsi ED. Treatment of human chronic lymphocytic leukemia cells with the proteasome inhibitor bortezomib promotes apoptosis. *Leuk Res* 2004; **28**: 845–850.
11 Matsumoto N, Ariga A, To-e S, Nakamura H, Agata N, Hirano S *et al.* Synthesis of NF-kappaB activation inhibitors derived from epoxyquinomicin C. *Bioorg Med Chem Lett* 2000; **10**: 865–869.
12 Ariga A, Namekawa J, Matsumoto N, Inoue J, Umezawa K. Inhibition of tumor necrosis factor-alpha-induced nuclear translocation and activation of NF-kappa B by dehydroxymethylepoxyquinomicin. *J Biol Chem* 2002; **277**: 24625–24630.
13 Cheson BD, Bennett JM, Grever M, Kay N, Keating MJ, O'Brien S *et al.* National Cancer Institute-sponsored Working Group guidelines for chronic lymphocytic leukemia: revised guidelines for diagnosis and treatment. *Blood* 1996; **87**: 4990–4997.
14 Andrews NC, Faller DV. A rapid micropreparation technique for extraction of DNA-binding proteins from limiting numbers of mammalian cells. *Nucleic Acids Res* 1991; **19**: 2499.
15 Horie R, Watanabe T, Morishita Y, Ito K, Ishida T, Kanegae Y *et al.* Ligand-independent signaling by overexpressed CD30 drives NF-kappaB activation in Hodgkin–Reed–Sternberg cells. *Oncogene* 2002; **21**: 2493–2503.
16 Romano MF, Lamberti A, Tassone P, Alfinito F, Costantini S, Chiurazzi F *et al.* Triggering of CD40 antigen inhibits fludarabine-induced apoptosis in B chronic lymphocytic leukemia cells. *Blood* 1998; **92**: 990–995.
17 Carew JS, Nawrocki ST, Krupnik YV, Dunner Jr K, McConkey DJ, Keating MJ *et al.* Targeting endoplasmic reticulum protein transport: a novel strategy to kill malignant B cells and overcome fludarabine resistance in CLL. *Blood* 2006; **107**: 222–231.
18 Morales AA, Olsson A, Celsing F, Osterborg A, Jondal M, Osorio LM. High expression of bfl-1 contributes to the apoptosis resistant phenotype in B-cell chronic lymphocytic leukemia. *Int J Cancer* 2005; **113**: 730–737.
19 Cuni S, Perez-Aciego P, Perez-Chacon G, Vargas JA, Sanchez A, Martin-Saavedra FM *et al.* A sustained activation of PI3K/NF-kappaB pathway is critical for the survival of chronic lymphocytic leukemia B cells. *Leukemia* 2004; **18**: 1391–1400.
20 Tallman MS, Hakimian D. Purine nucleoside analogs: emerging roles in indolent lymphoproliferative disorders. *Blood* 1995; **86**: 2463–2474.
21 Huang P, Sandoval A, Van Den Neste E, Keating MJ, Plunkett W. Inhibition of RNA transcription: a biochemical mechanism of action against chronic lymphocytic leukemia cells by fludarabine. *Leukemia* 2000; **14**: 1405–1413.

Retrovirology

BioMed Central

Research

Open Access

SUV39H1 interacts with HTLV-1 Tax and abrogates Tax transactivation of HTLV-1 LTR

Koju Kamoi[1,2], Keiyu Yamamoto, Aya Misawa[1], Ariko Miyake[1], Takaomi Ishida[1], Yuetsu Tanaka[3], Manabu Mochizuki[2] and Toshiki Watanabe*[1]

Address: [1]Laboratory of Tumor Cell biology, Department of Medical Genome Sciences, Graduate School of Frontier Sciences, The University of Tokyo, 4-6-1 Shirokanedai, Minato-ku, Tokyo 108-8639, Japan, [2]Department of Ophthalmology and Visual Science, Graduate School, Tokyo Medical and Dental University, 1-5-45 Yushima, Bunkyo-ku, Tokyo 113-8519, Japan and [3]Department of Immunology, Graduate School of Medicine, University of the Ryukyus, Okinawa 903-0215, Japan

Email: Koju Kamoi - koju1030@ims.u-tokyo.ac.jp; Keiyu Yamamoto - keiyu@ims.u-tokyo.ac.jp; Aya Misawa - ayamsw@ims.u-tokyo.ac.jp; Ariko Miyake - amiyake@ims.u-tokyo.ac.jp; Takaomi Ishida - tishida@ims.u-tokyo.ac.jp; Yuetsu Tanaka - yuetsu@ma.kcom.ne.jp; Manabu Mochizuki - m.manabu.oph@tmd.ac.jp; Toshiki Watanabe* - tnabe@ims.u-tokyo.ac.jp

* Corresponding author

Published: 13 January 2006

Retrovirology 2006, **3**:5 doi:10.1186/1742-4690-3-5

Received: 11 November 2005
Accepted: 13 January 2006

This article is available from: http://www.retrovirology.com/content/3/1/5

Abstract

Background: Tax is the oncoprotein of HTLV-1 which deregulates signal transduction pathways, transcription of genes and cell cycle regulation of host cells. Transacting function of Tax is mainly mediated by its protein-protein interactions with host cellular factors. As to Tax-mediated regulation of gene expression of HTLV-1 and cellular genes, Tax was shown to regulate histone acetylation through its physical interaction with histone acetylases and deacetylases. However, functional interaction of Tax with histone methyltransferases (HMTase) has not been studied. Here we examined the ability of Tax to interact with a histone methyltransferase SUV39H1 that methylates histone H3 lysine 9 (H3K9) and represses transcription of genes, and studied the functional effects of the interaction on HTLV-1 gene expression.

Results: Tax was shown to interact with SUV39H1 *in vitro*, and the interaction is largely dependent on the C-terminal half of SUV39H1 containing the SET domain. Tax does not affect the methyltransferase activity of SUV39H1 but tethers SUV39H1 to a Tax containing complex in the nuclei. In reporter gene assays, co-expression of SUV39H1 represses Tax transactivation of HTLV-1 LTR promoter activity, which was dependent on the methyltransferase activity of SUV39H1. Furthermore, SUV39H1 expression is induced along with Tax in JPX9 cells. Chromatin immunoprecipitation (ChIP) analysis shows localization of SUV39H1 on the LTR after Tax induction, but not in the absence of Tax induction, in JPX9 transformants retaining HTLV-1-Luc plasmid. Immunoblotting shows higher levels of SUV39H1 expression in HTLV-1 transformed and latently infected cell lines.

Conclusion: Our study revealed for the first time the interaction between Tax and SUV39H1 and apparent tethering of SUV39H1 by Tax to the HTLV-1 LTR. It is speculated that Tax-mediated tethering of SUV39H1 to the LTR and induction of the repressive histone modification on the chromatin through H3 K9 methylation may be the basis for the dose-dependent repression of Tax transactivation of LTR by SUV39H1. Tax-induced SUV39H1 expression, Tax-SUV39H1 interaction and tethering to the LTR may provide a support for an idea that the above sequence of events may form a negative feedback loop that self-limits HTLV-1 viral gene expression in infected cells.

Background

Human T-cell leukemia virus type 1 (HTLV-1) is the causative agent of an aggressive leukemia known as adult T-cell leukemia (ATL), as well as HTLV-1 associated myelopathy/tropical spastic paraparesis (HAM/TSP) and HTLV-1 uveitis (HU). These diseases develop usually after more than 40 years of clinical latency [1-4]. No or little, if any, viral gene expression can be detected in the peripheral blood of HTLV-1 carriers or ATL cells, indicating that HTLV-1 is infected latently *in vivo* [5,6].

The viral protein Tax plays a central role in the development of diseases mentioned above in HTLV-1-infected carriers. Tax can activate transcription of the HTLV-1 genome as well as specific cellular genes including inflammatory cytokines and their receptors and adhesion molecules. Tax also shows transforming activity when expressed in T lymphocytes and fibroblasts [7-10]. Tax is a 40-kDa nuclear phosphoprotein which is translated from a spliced HTLV-1 mRNA transcribed from the 3' portion of the genome. Tax regulates multiple cellular responses by its protein-protein interactions with various host cellular factors. In the regulation of transcription, Tax does not bind DNA directly but stimulates transcription from the HTLV-1 LTR and from the promoters of specific cellular genes by recruiting cellular transcription factors. Tax-mediated transcriptional regulation is based on its interaction with DNA-binding transcription factors such as members of the cyclic AMP response element binding protein/activating transcription factor (CREB/ATF), the nuclear factor-κB (NF-κB), and the serum response factor (SRF) and with two related transcriptional co-activators CREB binding protein (CBP) and p300.

In order to activate transcription of the HTLV-1 genome, nuclear Tax interacts with the CREB/ATF family of transcriptional activators, which bind to the viral long terminal repeat (LTR) [11-14]. The interaction of Tax with CREB and the CREB response elements in the LTR results in a CREB response element-CREB-Tax ternary complex [10]. Tax also binds directly to the KIX domain of the transcriptional co-activators CREB-binding protein (CBP) and p300 [15,16]. CBP and p300 are histone acetylases and acetylate substrates such as histones and transcription factors and may serve as integrators of numerous cellular signaling processes with the basal RNA polymerase II machinery [17,18]. This would, in turn, allow controlled regulation and interaction with many cellular transcription factors including CREB, NF-κB/Rel, p53, c-Myb, c-Jun, c-Fos, and transcription factor IIB in a signal-dependent and, sometimes, mutually exclusive fashion. In this context, Tax-mediated repression of transcription of some cellular genes are explained by functional competition between transcription factors and Tax [19]. A recent report that Tax interacts with a histone deacetylase (HDAC) [20] showed a novel mechanism by which Tax represses transcription of certain target genes. HDAC1 is likely to compete with CBP in binding to Tax and functions as a negative regulator of the transcriptional activation by Tax.

Reversible modification of core histones plays an important role in the regulation of gene expression, such as acetylation, phosphorylation and methylation [21,22]. These covalent modifications, alone or in combination, act as a scaffold for the recruitment of specific regulatory proteins or protein complexes that participate in certain downstream nuclear process including transcription, replication and repair [23]. Thus, it is thought that this "histone code" may serve to establish and maintain distinct chromosomal domains that are epigenetically transmitted [24,25]. Consistent with the histone code, it has been revealed that the methylation of histone H3 lysine 9 (H3 K9), a modification associated with transcriptionally silent heterochromatin, is critical for long-range chromatin regulatory processes [26,27]. Several enzymes are known to methylate H3 K9, such as murine SUV39H1 and G9a proteins [28,29].

Although regulation of histone acetylation by Tax through its physical interaction with histone acetylases and deacetylases has been reported, functional interaction of Tax with histone methyltransferases (HMTase) has not been studied. Here we examined the ability of Tax to interact with a histone methyltransferase SUV39H1 and studied the functional effects of the interaction on HTLV-1 gene expression. We report that Tax interacts with SUV39H1 *in vitro*, and that a stronger binding is observed when mutant proteins retain the C-terminal half of SUV39H1 encompassing the SAC (SET-associated Cys-rich) and SET domains of SUV39H1 [30,31]. Our data indicate that Tax interaction does not affect the methytransferase activity of SUV39H1, but induces a relocalization of SUV39H1 in the nuclei resulting in colocalization with Tax. Furthermore, co-expression of SUV39H1 with N-terminal deletion mutant of Tax resulted in cytoplasmic distribution of both proteins. We further demonstrate that SUV39H1 represses Tax transactivation of HTLV-1 LTR promoter activity depending on the Suv39H1 methyltransferase activity and revealed induction of SUV39H1 expression by Tax and tethering of induced SUV39H1 to the HTLV-1 LTR. These data suggest a possible negative feedback loop of HTLV-1 gene expression in infected cells, which may be one of the bases for the induction of HTLV-1 latency.

Results

HTLV-I Tax interacts with SUV39H1

To determine whether HTLV-1 Tax has the ability to interact with SUV39H1, we used GST pull-down and co-immunoprecipitation assays by transient transfection of

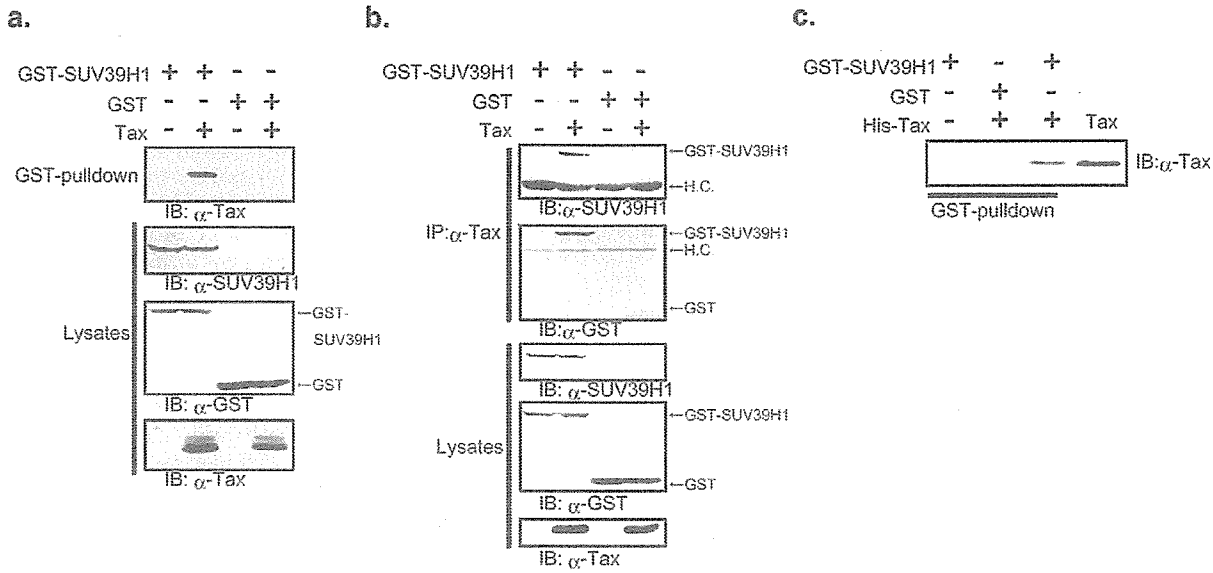

Figure 1

Tax interacts with SUV39H1 in vitro. (a) HEK293T cells were transiently cotransfected with GST-SUV39H1 or GST and Tax. After 48 h, the cells were lysed and the proteins were affinity purified with Glutathione Sepharose 4B. Purified proteins were separated by SDS-PAGE, transferred to a PVDF membrane, and probed with anti-Tax antibody Lt-4 (top panel). Expression of transduced proteins was confirmed by immunoblot analyses of whole cell lysates using respective antibodies (lower panels). (b) HEK293T cells were transiently co-transfected with expression plasmids, GST-SUV39H1 or GST and Tax. After 48 h, the cells were lysed and the proteins were immunoprecipitated with Lt-4. The immunoprecipitates were separated by SDS-PAGE, transferred to a PVDF membrane, and probed with anti-SUV39H1 or anti-GST antibody (upper panels). Expression of proteins was confirmed by immunoblot analyses of whole cell lysates using respective antibodies (lower panels). (c) Direct interaction between SUV39H1 and Tax. Bacterially expressed GST-SUV39H1 and GST were purified with Glutathione Sepharose 4B, and histidine-tagged wild type Tax (His-Tax) was purified with ProBond Resin (Promega). GST-SUV39H1 and GST were bound to Glutathione Sepharose 4B, and mixed with purified His-Tax in PBS. After centrifugation, proteins bound to Glutathione Sepharose 4B were separated by electrophoresis, transferred to a PVDF membrane, and probed with anti-Tax antibody. As a control, an aliquot of purified His-Tax was run in lane 4. IP, immunoprecipitation; IB, immunoblot; H.C., heavy chain

expression vectors for these proteins. Transient transduction was used for the experiments because the assays were not sufficiently sensitive with endogenous proteins and others also encountered this problem [32]. Expression vectors for the wild type HTLV-1 Tax (pCG-Tax) and GST-tagged SUV39H1 (pMEG-SUV39H1) were transfected into HEK293T cells as described in Materials and Methods. GST-SUV39H1 protein was affinity purified using Glutathione-Sepharose 4B column from total cellular proteins. Co-purified proteins were analyzed by immunoblotting using anti-Tax monoclonal antibody Lt-4 [33]. Total cellular proteins were also analyzed by immunoblotting as controls for protein expression using antibodies for SUV39H1, Tax and GST proteins. The results clearly showed that affinity-purified GST-SUV39H1 complex contained HTLV-1 Tax protein, whereas Tax protein was not co-purified with GST alone (Figure 1a). Conversely, when the cell lysates were immunoprecipitated with anti-Tax antibody Lt-4, the immune complex was shown to contain SUV39H1 that was detected by anti-SUV39H1 antibody as well as anti-GST antibody (Fig. 1b, upper two panels). Absence of Tax protein in the immune complex when GST protein alone was co-expressed denied the possibility that Tax might be co-immunoprecipitated because of the affinity to GST protein (Fig. 1b, lane 4). Taken together, these results suggested that wild type Tax interacts with SUV39H1 in cultured cells.

Next, we examined direct interaction between Tax and SUV39H1 using bacterially expressed and purified proteins. GST pull-down assays of histidine-tagged Tax and GST-fusion SUV39H1 were performed for this analysis.

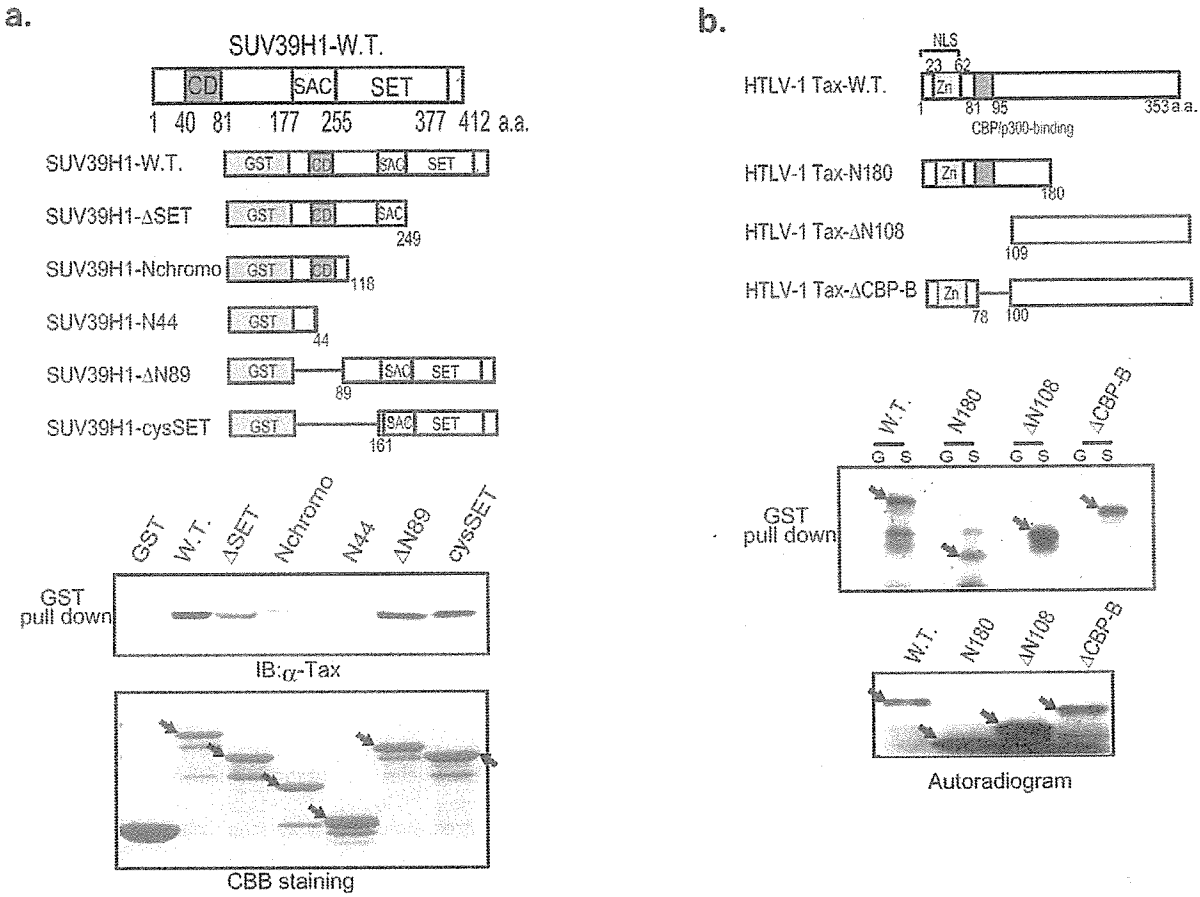

Figure 2

Analyses of the interacting domains. (a) GST pull-down assays using bacterially expressed GST-tagged wild type and various mutants of SUV39H1 and histidine-tagged wild type Tax (His-Tax). A schematic representation of the wild type (SUV39H1-WT) and those of domain structures of mutants are indicated in the upper panels. Results of the pull-down assays are shown in the lower panels. Pulled-down proteins were analyzed by SDS-PAGE and immunoblotting with Lt-4 antibody (top of the lower panels). The bottom panel shows the Coomassie Brilliant Blue (CBB)-stained gel where the wild type and various mutant SUV39H1 proteins were run. (b) Pull-down assays using the wild type GST-SUV39H1 and *in vitro* translated wild type and various mutant Tax proteins. Schematic description of the structures of wild type and various mutant Tax proteins is presented in the top panel. Results of the pull-down assays are shown in the top of the lower panels. Pulled-down Tax proteins that were labeled with ^{35}S-methionine were visualized by autoradiography (top of the lower panels). The bottom panel shows the autoradiogram of the gel where the radio labeled wild type and various mutant Tax proteins were run.

The results clearly showed that Tax protein directly interacts with GST-SUV39H1 but not with GST protein alone (Fig. 1c).

Binding domain analysis

To define the domains within SUV39H1 and Tax that are responsible for the interaction, we performed *in vitro* binding assays. First, we constructed various mutants of SUV39H1 according to the domain structure [34] (Fig. 2a, upper panel) and examined binding to the His-tagged wild type Tax protein that was bacterially expressed and purified by ProBond Resin (Promega). When C-terminally deleted series of SUV39H1 were examined, a mutant (ΔSET) that lost the SET domain and the C-terminal cysteine-rich region, but retained the SET-associated Cys-rich (SAC) domain, showed a significantly decreased binding (less than half of the band intensities of the wild type, ΔN108 and ΔCBP-B, when measured by NIH Image software). Further deletion up to amino acid 118 that resulted in loss of the SAC domain (a mutant named

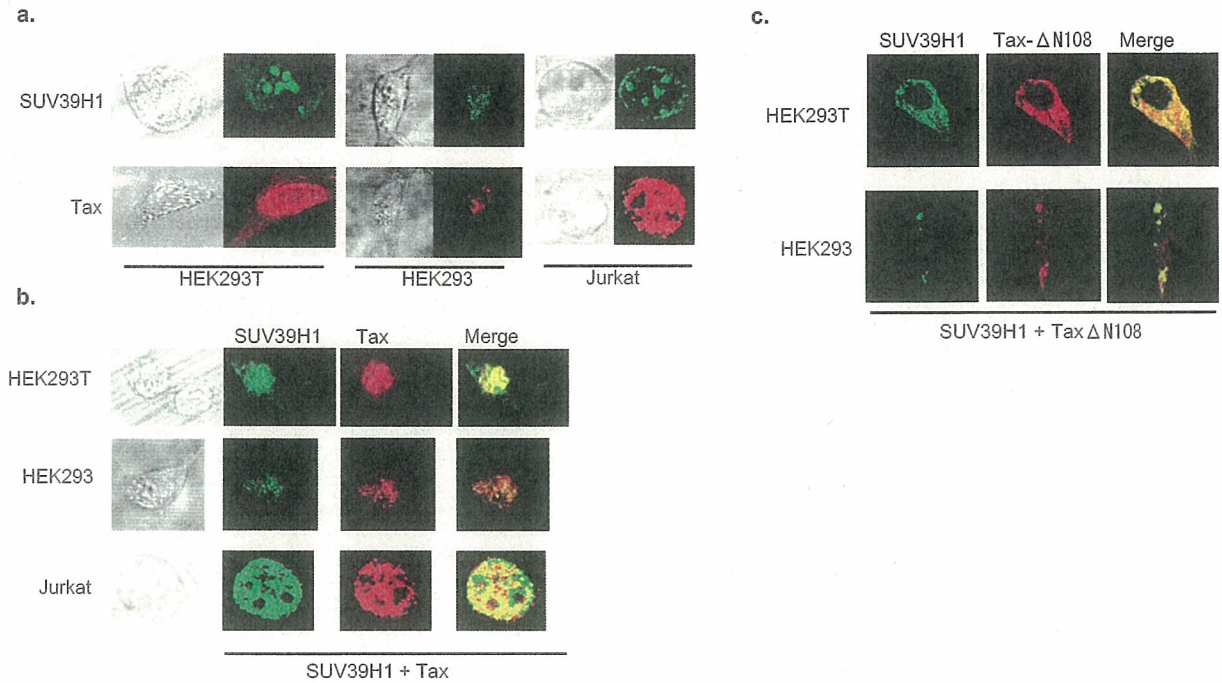

Figure 3
Immunofluorescence microscope analysis of SUV39H1 and Tax. (a) HEK293T, HEK293 and Jurkat cells were cultured on glass coverslips, transfected with SUV39H1 or Tax (upper and lower panels, respectively). Large and defined nuclear speckles were observed in the cells transfected with SUV39H1 (upper panels). Rather diffuse nuclear localization was observed in those transfected with Tax (lower panels). Phase contrast photographs are on the left of each immunofluorescence photograph. (b) HEK293T, HEK293 and Jurkat cells transfected with SUV39H1 and Tax expression plasmids together. Phase contrast photographs are on the left of immunofluorescence photographs. The merged photographs are shown on the right of each panel. (c) HEK293T and HEK293 cells transfected with SUV39H1 and TaxΔN108 together. The merged photograph is shown on the right.

Nchromo) showed very weak residual binding activity (about one tenth of the intensities of the wild type, ΔN108 and ΔCBP-B). A mutant retaining only the N-terminal 44 amino acids (N44) totally lost binding activity (Fig. 2a, top of the lower panels, lanes 2 to 5). Two N-terminally deleted mutants (ΔN89 and cycSET) were tested to narrow down the binding region. The ΔN89 mutant lacks the N-terminal region including the chromodomain but retains the region between the chromodomain and the SAC domain (amino acids 89 to 160). The cycSET mutant retains the SAC and SET domains with the C-terminal cysteine-rich region. GST pull-down assays showed that both mutants have strong binding activities, indicating that the loss of the amino acids from 89 to 160 does not affect binding activity. Taken together, although the interaction appears to be complex and may involve several domains, the region of amino acids from 161 to 412 (the SAC-SET domains and C-terminal cysteine-rich region) appears to be enough to show a high affinity for Tax protein. Since the defined region comprises the catalytic motif required for the HMTase activity [34], the results shown above indicate that the catalytic region of SUV39H1 appears to play an important role in the interaction with Tax.

We then analyzed the domains of Tax protein responsible for the interaction with SUV39H1. In addition to the wild type Tax, we used three kinds of mutants, TaxN180, TaxΔN108 and ΔCBP-B. TaxN180 has a C-terminal deletion up to 180 amino acids, TaxΔN108 a deletion of N-terminal 108 amino acids and ΔCBP-B a deletion of the CBP binding domain (amino acids from 79 to 99) (Fig. 2b, upper panel). After *in vitro* translation and labeling with ^{35}S-Methionine, the wild type Tax and these mutants were used for *in vitro* pull-down assays with GST-SUV39H1. The results demonstrated that the wild type Tax and all these mutants can bind to SUV39H1 (Fig. 2b, top of the lower panels). However, TaxN180 showed a significantly weaker binding compared with other proteins (about half of the radioactivity of the wild type Tax), suggesting that

the C-terminal region of Tax may have a higher affinity for SUV39H1. Furthermore, it was shown that the p300/CBP-binding domain is dispensable for the interaction with SUV39H1 (Fig. 2b, top of the lower panels).

Co-localization of Tax and SUV39H1 in vivo

Next, we examined by confocal immunofluorescence analysis whether the intracellular localization of SUV39H1 may be influenced by interaction with Tax. When SUV39H1 alone was transduced in HEK293T, HEK293 and Jurkat cell lines, it showed large and defined nuclear speckles as reported previously [32,35] (Fig. 3a, upper panel). It is known that Tax usually shows speckled nuclear distribution [36,37], whereas in another report it shows diffuse nuclear localization [38]. In our experiments using HEK293T and Jurkat cells, transduced Tax showed diffuse nuclear localization similar to the previous report [38]. (Fig. 3a, lower panel). However, when these two proteins were simultaneously transduced, SUV39H1 protein did not show the speckled distribution and was diffusely distributed within the nuclei and colocalized with transduced Tax in all these cell lines (Fig. 3b). Since the distribution of Tax protein did not appear to have changed in the cells where both proteins were co-expressed, the results suggest a tethering of SUV39H1 by Tax.

To examine the possible tethering of SUV39H1 by Tax, we transduced an N-terminally deleted mutant Tax protein (TaxΔN108) lacking the nuclear localization signal and the wild type SUV39H1 in HEK293T and HEK293 cell lines. Transduced TaxΔN108 showed a clear cytoplasmic distribution as expected (Fig. 3c). In the presence of TaxΔN108, co-expressed SUV39H1 showed a cytoplasmic distribution instead of the nuclear localization seen when expressed alone (Fig. 3c). These results provide supportive evidence for the idea that Tax influences the cellular localization of SUV39H1.

SUV39H1 methyltransferase activity is not affected by the interaction with Tax

When two proteins interact with each other, functional modulation is expected to take place. Thus, we first examined whether association with Tax may affect the HMTase activity of SUV39H1, using *in vitro* methyltransferase assays according to the method reported by Fuks et al. with slight modifications [39]. First, we measured methyltransferase activities of immunoprecipitated SUV39H1 alone that was transduced in HEK293T cells, and studied the time course of the activities (Fig 4a). SUV39H1 immunoprecipitates methylated the substrate H3 (Fig. 4a, top panel). The levels of methylation appeared to become saturated at 60 min and thereafter (Fig. 4a, middle panel). Thus, we performed the reaction for 30 min to examine the effects of Tax on SUV39H1 HMTase activities. When

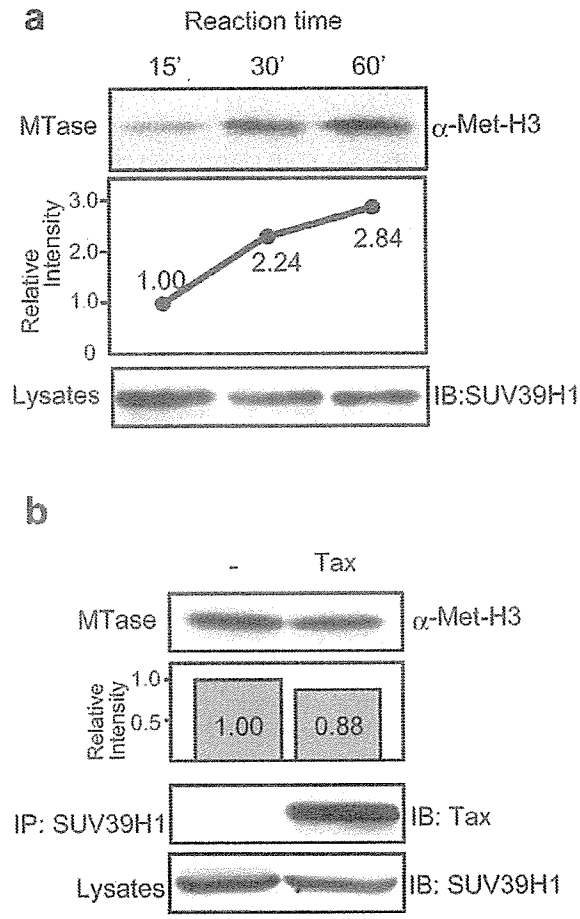

Figure 4

Results of *in vitro* methyltransferase assays. (a) Time course analysis. Top panel shows a representative fluorogram of the reaction mixtures at the indicated time points analyzed by 15% SDS-PAGE. The middle panel shows the relative levels of methylation measured by densitometric analyses of the bands. Bottom panel, a result of immunoblot analysis of transduced SUV39H1 by anti-SUV39H1 monoclonal antibody, showing comparable levels of SUV39H1 expression in each sample. (b) A representative result of three independent experiments of *in vitro* methyltransferase assays of SUV39H1 transduced with or without Tax. The reaction time was 30 min. The second panel shows the relative intensities of the methylated H3 bands. Lower panels show the results of immunoblot analyses of the immunoprecipitates and whole cell lysates to show the presence of SUV39H1 with or without Tax. IP, immunoprecipitation; IB, immunoblot. Antibodies used are indicated on the side of the panels.

Tax was co-expressed with SUV39H1 in HEK293T cells, the immunoprecipitates showed almost equal levels of methyltransferase activities compared with that of singly

expressed SUV39H1 (Fig. 4b, upper two panels). Taken together, these results suggest that although Tax shows a high affinity for the region containing the SET domain of SUV39H1, Tax does not affect the HMTase activity of SUV39H1 under the experimental condition used.

SUV39H1 represses Tax transactivation of HTLV-I LTR promoter activity

Since Tax interacts with and tethers SUV39H1 without affecting HMTase activity, it is possible that SUV39H1 associated with Tax will methylate H3 K9 of the local chromatin where Tax is located, resulting in an interference of Tax function. One of the main biological functions of Tax is transcriptional transactivation of HTLV-1 LTR leading to efficient expression of viral RNA and viral replication in the infected cells. Thus, we examined the effects of SUV39H1 on transactivating function of Tax using pHTLV-LTR-Luc as a reporter. When transduced alone, Tax transactivated the HTLV-1 LTR promoter activity more than 200- and 20-fold in HEK293 and Jurkat cells, respectively. However, when SUV39H1 was co-transduced with Tax, the transactivation was dose-dependently suppressed in both cell lines down to the baseline levels with 500 ng or 1000 ng of the SUV39H1 plasmid (Fig. 5a, left and right panels). On the other hand, SUV39H1 alone showed only a little suppressive activity on the basal activities of HTLV-1 LTR promoter in both cell lines with corresponding amounts of the expression plasmid in the above experiments (Fig. 5b, left and right panels).

Next, we tested whether repression of Tax transactivation by SUV39H1 is dependent on the SUV39H1 methyltransferase activity. For this purpose, we used a loss-of-function mutant of SUV39H1 (H324L) reported by Lachner et al. [40], as well as deletion mutants used for the binding analysis. Co-expression of SUV39H1 (H324L) with Tax did not show a significant suppression of Tax transactivation of HTLV-1 LTR promoter activity (Fig. 5c). Furthermore, co-expression of C-terminal deletion mutants of SUV39H1 (ΔSET, Nchromo and N44) did not show any suppression of Tax transactivation, whereas co-expression of deletion mutants retaining the SAC-SET region (ΔN89 and cysSET) showed suppression of Tax transactivation similar to the levels by the wild type SUV39H1 (Fig. 5c).

Taken together, these results indicate that the interaction between SUV39H1 and Tax leads to repression of Tax transactivating function on HTLV-1 LTR depending on the HMT activity of SUV39H1.

Induction of SUV39H1 expression by Tax and localization on HTLV-I LTR

Above results suggest that SUV39H1 may be a cellular protein counteracting with Tax function. Thus, we next tested the possibility that SUV39H1 expression may be induced by Tax, using JPX9 cells where Tax expression can be induced by $CdCl_2$ [41]. As was previously reported, treatment of JPX9 cells with $CdCl_2$ resulted in a strong induction of Tax, which was associated with SUV39H1 expression (Fig. 6a, upper figure, upper two panels). Since $CdCl_2$ treatment of Jurkat cells, from which JPX9 cells were derived, did not show any effects on the levels of SUV39H1 expression (Fig. 6a, lower figure), SUV39H1 appears to be induced by Tax as one of the Tax target genes.

Next, we examined whether Tax-induction of SUV39H1 leads to localization of SUV39H1 on the HTLV-1 LTR by chromatin immunoprecipitation (ChIP) assays using stable transformants of JPX9 cells transfected with the HTLV-1 LTR Luc plasmid (JPX9LTR clones). PCR analysis showed a clear difference between the ChIP samples of $CdCl_2$ treated (48 h) and untreated JPX9LTR clones (Fig. 6b, top panel). The intensity of the band was almost 10-fold stronger in $CdCl_2$ treated JPX9LTR cells than that of untreated cells measured by NIH Image software (Fig. 6b, second panel). The intensity of the PCR product from the $CdCl_2$ untreated JPX9LTR clones was almost the same as those from the samples of negative control without anti-SUV39H1 antibody (Fig. 6b). These results suggest that, with the induction of Tax expression, at least part of the induced SUV39H1 protein is recruited to the HTLV-1 LTR sequence. Detailed analyses of JPX9LTR clones as to time course of LTR promoter activities, protein expression levels, intracellular localization and so on are now under way in our laboratory, which will be reported in a separate paper.

To examine whether HTLV-1-infected cells express higher levels of SUV39H1, we studied SUV39H1 expression in T cell lines derived from ATL cells (TL-om1 and MT-1) as well as in those without HTLV-1 infection (Jurkat and CEM). The results clearly showed higher levels of SUV39H1 expression in ATL-derived T cell lines compared with T cell lines without HTLV-1 (Fig 6c, upper panel). These results suggest that SUV39H1 is one of the cellular target genes of Tax.

Discussion

Tax is a multi-functional regulatory protein encoded by HTLV-1. Through a protein-protein interaction, Tax deregulates multiple cellular processes including cell cycle progression, signal transduction and transcriptional regulation, which provide bases for HTLV-1 pathogenicity. In the present study, we demonstrated for the first time the interaction between HTLV-1 Tax and a histone methyltransferase SUV39H1. The interaction was largely dependent on the C-terminal half of the SUV39H1 protein that encompasses the SAC and SET domains and the

C-terminal cysteine-rich region. Interaction with Tax did not affect the SUV39H1 HMTase activity in *in vitro* methyltransferase assays. Tax tethered SUV39H1 resulting in colocalization with Tax in the nuclei and in the cytoplasm when an NLS (-) Tax mutant was expressed. These data provide strong supportive evidence for the idea that Tax directs the cellular localization of SUV39H1. Reporter gene assays showed that transduction of SUV39H1 represses Tax transactivation of HTLV-1 LTR promoter activity, which is dependent on the HMTase activity. Furthermore, endogenous SUV39H1 expression appeared to be induced by Tax expression in JPX9 cells, and induced SUV39H1 was shown to be recruited to the HTLV-1 LTR. Taken together, these data may suggest a negative feedback loop of HTLV-1 gene expression in the infected cells, where the transcriptional activator Tax itself may serve as a trigger for a self-limiting control over viral gene expression through the recruitment of SUV39H1 to HTLV-1 LTR and inducing H3 K9 methylation and a repressive histone code on the LTR.

By GST pull-down experiments, the Tax binding domain of SUV39H1 was narrowed down to the region covering the SAC and SET domains (Fig. 2a). On the other hand, the SUV39H1 binding domain of Tax was not clearly defined because all Tax mutants used showed affinities for SUV39H1 (Fig. 2b). However, the results indicated that the N-terminal region of about 100 amino acids of Tax is not essential for a high affinity interaction with SUV39H1 (Fig. 1b). This region contains the nuclear localization signal (NLS) and the CBP binding domain (CBP-B) [38,42]. The CBP-B of Tax does not appear to be involved in the binding to SUV39H1, since the amounts of the pull-down products of the mutants lacking this region (ΔCBP-B and TaxΔN108) were almost equal to that of the wild type (Fig. 2b), and co-expression of SUV39H1 with TaxΔN108 lacking NLS showed cytoplasmic localization of SUV39H1 (Fig. 3c). Many functional domains reside in the region where Tax shows a higher affinity for SUV39H1, such as those involved in the interaction with IKKγ [43], self-dimerization [44], and Rev-like nuclear export signal [45]. Thus, although SUV39H1 shares a functional characteristic with p300/CBP as histone modification enzymes, it appears to interact with Tax in a region distinct from that of p300/CBP. Consequently, the competition model proposed for repression of Tax transactivation by p53 may not be the mechanism by which SUV39H1 represses Tax transactivation.

Tax binding domain of SUV39H1 appears to be located in the C-terminal half region encompassing the SAC-SET and the C-terminal cysteine-rich regions (Fig. 2a). Our results contrast with previous reports showing that the N-terminal region of SUV39H1 is involved in the interaction with other proteins such as HP1b, HPC2, HDAC1 and 2 [31,32,46]. The interaction between SUV39H1 and the above proteins provides a scaffold for a functional multiprotein complex [39,47,48]. Furthermore, the N-terminal domain of 3–118 amino acids is considered the heterochromatin-targeting region. On the other hand, the SET domain is considered a dominant module which regulates SUV39H1 function such as chromatin distribution and protein interaction potentials [31]. The finding that interaction with Tax does not affect HMT activity of SUV39H1 (Fig. 4b) may suggest a new potential to form Tax-containing protein complexes in which above mentioned functions of SUV39H1 are preserved.

It was reported that endogenous SUV39H1 is a heterochromatic protein during interphase that selectively accumulates at centromeric positions of metaphase chromosomes [29,49]. Furthermore, the chromosomal localization of human SUV39H1 is very sensitive to protein expression levels [31]. In the present study, co-expression experiments showed a re-localization of nuclear SUV39H1, losing its typical speckled pattern in the presence of Tax (Fig. 3). SUV39H1 shows a rather diffuse distribution and co-localization with Tax in all cell lines used. These results suggest a possibility that Tax tethers SUV39H1 to the region where Tax is localized (Fig. 3b). This notion is supported by the observation that a mutant Tax lacking the NLS directs cytoplasmic localization of SUV39H1 (Fig. 3c). High levels of expression and coexistence of these proteins can be expected in the cells soon after HTLV-1 infection where the viral gene is vigorously transcribed and abundant Tax protein presumably coexists with high levels of SUV39H1 protein induced by Tax. If Tax tethers SUV39H1, Tax and SUV39H1 may form a repressive complex at the promoter where Tax is localized, thereby SUV39H1 may counteract the transcriptional activation by Tax. Our results of reporter gene assays and ChIP analysis showing dose-dependent repression of Tax transactivation of HTLV-1 LTR and SUV39H1 recruitment to the LTR after Tax induction in JPX9LTR cells provide a supportive evidence for this hypothesis. Thus, a negative feedback loop can be conceived by which HTLV-1 gene expression is made self-limiting. Since SUV39H1 can interact and form a complex with DNA methyltransferases [39], demonstration of SUV39H1 complex on HTLV-1 LTR may also provide a basis for the mechanism of heavy CpG methylation of HTLV-1 LTR in the latently infected cells in the peripheral blood and ATL cells *in vivo* [5].

Conclusion

In the present paper we demonstrated for the first time the interaction between SUV39H1 and HTLV-1 Tax, and apparent tethering of SUV39H1 by Tax, leading to co-localization in the nuclei. Since Tax interaction does not affect SUV39H1 HMTase activity, Tax-mediated tethering of SUV39H1 to the LTR and induction of a conforma-